Response to Reviewer 1

We would like to thank the anonymous reviewer for his or her constructive comments. In this response we provide an answer to all the comments and then indicate the changes that are applied in the revised manuscript. All line numbers we will refer to are based on the revised manuscript (not the marked-up manuscript).

Comment 1: *My major concern is about the validity of one assumption in the model. I am not fully convinced and expect a better justification. Because the model does not represent the river routing process, it uses floodplain connectivity to simulate the transport of sediment along hydrological pathways. However, by doing so, it implicitly assumes all sediments as sand and gravels (non-cohesive sediment) and represents the transport of cohesive and non-cohesive sediment in the same way. But the cohesive sediments (loam and silt) can be transported by rivers efficiently and most of them would not be deposited. Further, loam and silt may be the major type of sediments that are generated from hillslope erosion (especially for interrill and rill erosion considered by RUSLE). As shown in the results, the current method can cause the severe underestimation of sediment and C that are transported to oceans.*

Answer: We understand the reviewer's concern regarding the absence of an explicit representation of rivers and river routing in CE-DYNAM. We agree that in this way we treat the transport of all sediments types (cohesive and non-cohesive) in the same way, which can lead to uncertain sediment and POC fluxes carried away by rivers. However, our model assumption does not imply that all sediments are in the form of coarse material, instead, the main assumption is that the majority of the eroded soil and transported sediment is fine sand, silt and loam. This assumption is supported by the fact that the sediment residence time is calculated based on observed floodplain deposit ages of the Rhine (Hoffmann et al. 2007, 2008, 2013). These studies show that most of the deposits in the floodplains are overbank deposits that consist of fine sediment such as sand, loam, silt and clay and organic material. The long residence time (up to 2000 years) that they measured for the floodplains based on the C14 signature of C associated

with sediment samples show that the fine sediment can stay buried for a long time in the floodplains. Although the model lacks explicit river process representations, it reproduces the spatial variability in floodplain sediment and C storage across the Rhine sub-basins as is shown by table 3 of this manuscript and by a previous study where we validated the global sediment budget model (Naipal et al., 2016, ESD). It should be noted that the model has been developed and calibrated to simulate long-term changes in sediment and carbon storage on land and not the short-term variations in sediment and POC fluxes carried by rivers.

Finally, the model produces a sediment export flux at the end of the year 2005 of $1.6x10^7$ tonnes per year, which is a magnitude higher than the measured suspended sediment flux of about $3.15x10^6$ tonnes per year (Asselman et al.,2003). The higher sediment flux is the result of absent riverine processes in CE-DYNAM such as sediment burial behind dams, and the fact that we assume an equilibrium state for the Rhine catchment based on the period 1850-1860 where agricultural soil erosion rates were already high. The simulated total cumulative sediment export of 2.5 Gt for the Rhine over the period 1850-2005 is about 36 % of the cumulative gross soil erosion flux of 6.8 Gt. This sediment flux leads to a cumulative POC export of about 0.14 Tg of C for the Rhine over the period 1850-2005 (based on a new simulation S2, see more details in the following paragraph below). This is 0.2 % of the cumulative C erosion flux. The yearly POC flux at the end of the year 2005 is 0.02 tC km^2 $year^{-1}$ (normalized over the total basin area), which is an order of magnitude lower compared to other studies who found 0.9 tC km^2 $year^{-1}$ (Beusen et al., 2009; Soribas et al., 2016).

This underestimation in POC in CE-DYNAM is most likely a result of the high sediment residence time of floodplains downstream of the Rhine and the absence of increased plant productivity of floodplains, leading to the decomposition of a large fraction of the deposited C. We tested the effect of the sediment residence time on the resulting lateral C fluxes of the model and find that they do not change the POC export of the Rhine significantly (see our detailed response to comment 2 of reviewer 2). Increased plant productivity of floodplains is shown to contribute significantly to the higher SOC stocks of floodplains compared to hillslopes, and to the export of DOC and POC to rivers (Van Oost et al., 2012; Hoffmann et al., 2013).

Changes to the manuscript: See lines 703-724 of section 4.2 of the revised manuscript.

New transient simulation S2 based on an improved equilibrium state

We redid the simulation S2 for the Rhine catchment using a different model spin-up. In the old spin-up we let the model run continuously for 2000 years, whereas in the new spin-up we ran the model for 3000 years and calculated analytically the temporary equilibrium state of the floodplain SOC pools every 10 years. This new spin-up method resulted in the floodplain SOC pools being close to equilibrium at the end of the 3000 year spin-up period, where the yearly change in the floodplain SOC stocks was less than 0.001% of the total floodplain SOC stock. Therefore, it was not needed to subtract the additional increase in the SOC stocks resulting from the disequilibrium state from those of the transient simulation (see section 2.11). The new transient simulation S2 resulted in different absolute values for the C budget of the Rhine. However, the main conclusions did not change. We also performed an uncertainty analysis with a minimum and maximum soil erosion scenario, based on the uncertainty ranges in the rainfall erosivity and land cover factors of the Adjusted RUSLE model. The revised manuscript will contain the adapted figures and tables. In addition, section 3 is modified to include the new results with uncertainty ranges.

Changes to the manuscript: See lines 436-439 of section 2.11 of the revised manuscript.

Specific comments

Comment S1: *L70-72: These two references are relevant to this sentence.*

Galy, V., Peucker-Ehrenbrink, B., & Eglinton, T. (2015). Global carbon export from the terrestrial biosphere controlled by erosion. Nature, 521, 204–207.https://doi.org/10.1038/nature14400

Tan, Z., Leung, L. R., Li, H., Tesfa, T., Vanmaercke, M., Poesen, J., ... Hartmann, J. (2017). A Global data analysis for representing sediment and particulate organic C carbon yield in Earth

System Models. Water Resources Research, 53, 10,674–10,700. https:// doi.org/10.1002/2017WR020806

Answer: We added these references in the revised manuscript

Changes to the manuscript: See lines 72-73 of the introduction of the revised manuscript.

Comment S2: *L117: it should be noted that as discussed in Naipal et al. (2015), the formulation of R factor is related to climate type. So in the millennia time scale, one area may need different R factors due to the change of climate.*

Answer: This is right. In the paper of Naipal et al. (2016), where the global sediment budget model is applied for the last millennium, we take the change in climate in the calculation of the erosivity into account. For this study, we assume that the climate zones as defined by the Koeppen-Geiger climate classification have not changed drastically since 1850 AD.

Changes to manuscript: See lines 142-144 of section 2.2 of the revised manuscript.

Comment S3: *L170: Reference for Eq. 5? Also, I recommend to show the spatial variability of the f factor in the Rhine catchment.*

Answer: This equation has been adopted from the study of Naipal et al. (2016), that presents the global sediment budget model for the Rhine. We included the reference to this equation in the revised manuscript and added the spatial variability of the f factor in the supplementary document.

Changes to manuscript: See line 172 of section 2.3 in the revised manuscript and section S1 and S2 of the supplementary document.

Comment S4: *L192: This may be true for sand and gravel sediment (the majority of floodplain sediment) that Hoffmann et al. (2008) studied. But for cohesive sediment (loam and silt), they can be transported through river channels to oceans without the large fraction of deposition (at least not as large as what is set in this model). They are also the major sediments of soil erosion.*

Answer: See our answer to the previous comment, where we argue that most of the floodplain sediment studied by Hoffmann et al. (2008) consists mostly out of organic material (gyttja, peat) and fine sediments (fine sand, loam, silt) in overbank deposits (see table 2 in Hoffmann et al., 2008). These fine sediments are a result of long-term soil erosion on the hillslopes. Also a large part has been transported and deposited in the floodplains under major storms, such as the one in the 14th century (Bork et al., 2003). In this study (Table 6, and section 3.1 of the revised manuscript) and a previous study on the millennial sediment storage of the Rhine (Naipal et al., 2016) we show that by getting the scaling relationships as found by Hoffmann et al. (2013) right, the sediment residence time is realistic.

To show the potential effects of a different sediment residence time on the SOC storage and POC flux, we performed a sensitivity study where we changed the basin average sediment residence time to be 50% higher or 50% lower but keeping the maximum sediment residence time at 1500 years. We find that the POC flux under the low sediment residence time scenario is substantially higher than under default conditions compared to default conditions. However, the impacts of a modified sediment residence time on the total SOC storage of the Rhine are non-linear. The results of this sensitivity study is summarized in the new table 7 and in the discussion section of the revised manuscript. See changes to the manuscript and our response to reviewer 2, where we describe in the model sensitivity analysis in more detail.

Changes to manuscript: See lines 447-450 of section 2.11, lines 411-414 of section 2.10, and lines 790-807 of the new section 4.3 in the revised manuscript. See also the new table 7.

Comment S5: *L202: Similar above, this routing scheme may be fine for floodplain but whether it is appropriate for river sediment routing is questionable. And river sediment routing transports large amounts of sediment and POC from hillslopes to oceans.*

Answer: See our response to comments 1 and S1

Comment S6: *L322-326: Could you make the meanings of each term in RHS of these equations*

*more clearly? Especially, I do not very understand what the second term of RHS of Eq. 16 stand for. Also in Eq. 17, what is the difference between 1/(τ *365) and kiout for SOCFLi(0,t) in the third term?*

Answer: The second term at the RHS of Eq. 16 stands for the C flux flowing into soil layer z from the soil layer z+1 below, and is related to the C export flux of the floodplain part of a grid cell. When the topsoil layer loses C due to sediment routing, the C from the subsoil layer 'moves' upward as is also done for C loss due to soil erosion (section 2.7). In Eq. 17 ki_{out} stands for the C import rate from the neighboring grid cells. We provided a short explanation of each term in the equations 16 and 17 in the revised manuscript.

Changes to manuscript: See lines 366-376 of section 2.8 in the revised manuscript.

Comment S7: *L431-432: Or as argued by Tan et al. (2018), rainfall erosivity itself tends to be less variable if using large scale rainfall data to calculate it.*

Answer: We agree with this statement, however, we removed figure 4 and its explanation in the revised manuscript as we think that it does not show any new results and is thus not needed.

Comment S8: *L455: could the map of these 13 sub-basins be shown?*

Answer: We included a map of the sub-basins of the Rhine catchment in the supplementary information.

Changes to manuscript: See section S3 of the supplementary document

Comment S9: *L471-473: if much more sediment was generated but sediment deposition may still follow the long-term level, where did this additional sediment go? I suspect that it mostly was transported to oceans, a process not or poorly represented in the current model.*

Answer: We agree that a large part of the sediment is transported out of the catchment, more specifically 36% of the cumulative gross soil erosion rates over the entire period (see our response to the first comment).In contrast, the largest part of the eroded C in either buried in deposition areas or respired. We aim to explicitly represent riverine processes in a future study

on the further development of CE-DYNAM where we also plan to include the impact of dams on the sediment export. However, the focus of this study lies on the redistribution of soil and C on land and their effect on the land-atmosphere C exchange, rather than on the riverine export fluxes of sediment and C.

Comment S10: *L474: that only 0.2% of sediment is exported out of the catchment is too low to believe. Are there any data to support it?*
Answer: See our answer to comment 1

Comment S11: *Section 4.2: The model also does not represent the impact of water management (such as flooding control) on floodplain connection.*
Answer: This is correct. We assume a 'natural' state of the catchment where the main river channel is not managed and the floodplains are more or less dynamic. We will specify this in the revised manuscript.
Changes to manuscript: See lines 722-723 of section 4.2 of the revised manuscript

Comment S12: *Figures: As discussed above, I recommend to add a few more figures (in either supplementary or appendix) to show the 13 sub-basins of the Rhine catchment and the spatial variability of the floodplain factor f and the sediment residence time* τ .
Answer: We added these figures in the supplementary info, see sections S1,S2 and S3 in the supplementary document

Comment S13: *Figure 2: What does the gray level stand for? Elevation?*
Answer: The gray level stands for elevation, where the darker colors represent higher elevations.
Changes to manuscript: We added this information in the figure caption of the revised manuscript.

Comment S14: *Figure 3: What does the x-axis mean? Why do not you do a cell-to-cell comparison instead?*

Answer: The x-axis represents bins or evenly spaced ranges between the minimum and maximum total yearly soil erosion rates of the Rhine. A cell-to-cell comparison does not show a clear result due to the large variability in erosion rates. We find a quantile plot like figure 3 more useful to see for which erosion ranges the rates differ significantly between the models.

Changes to manuscript: We adapted the figure captions of figure 3 and 4 to include the information on the bins.

Comment S15: *Figure 4. Do you have another way to convey the message? It looks messy currently.*

Answer: We agree that this figure does not convey the message properly, after reviewer 2 had a similar opinion. We also think that the figure is not very important.

Changes to manuscript: We removed this figure from the manuscript

Comment S16: *References: Generally good. I recommend to also acknowledge the progress in other groups to represent soil erosion at large scale numerical models, such as Pelletier (2012) and Tan et al. (2018).*

Changes to manuscript: We acknowledged these studies in the introduction.

Response to Reviewer 2

We would like to thank the anonymous reviewer for his or her constructive comments. In this response we provide an answer to all the comments and then indicate the changes that are applied in the revised manuscript. All line numbers we will refer to are based on the revised manuscript (not the marked-up manuscript).

Comment 1: *First of all the paper lacks clear aims (or research questions). In Line 68 to 83 the authors give an overview of the contents of the paper, but I think the entire paper would improve substantially if clear aims would be given here. For example, (i) introduce a coupled soil erosion and C turnover model with an LSM model which is applicable on regional scales. (ii) Rigidly test the model for the Rhine Catchment against other modelling results and regionally available data. (iii) Analyze the sensitivity/uncertainty of the model results due to weak input data and a priori model assumptions. (regarding (iii) see comments below.*

Answer: We clarified the aims of our study in the Introduction section of the revised manuscript. See changes below.

Changes to manuscript: Lines 78-91 of the revised manuscript

Comment 2: *Taking the temporal and spatial scale into account which should be later on analyzed with the model I think the authors found a good balance between model complexity and simplicity. However, the model is full of a priori assumptions, which will fundamentally affect the modelling results, so I personally do not think any model results can be interpreted without some estimates of at least the sensitivity of the model against these assumptions. The most important assumptions which could be tested easily are: C input via plants especially crops depending on erosion status, C enrichment during erosion and depletion during deposition, reduced C turnover in alluvial soils due to wetter conditions, etc. Overall, it is one of the major shortcomings of the paper that the modeling results in section 3.2 are presented single values (e.g. for 159 Tg C for C removal by erosion) and also conclusions based on this single model*

results are presented. I strongly suggest performing a a sensitivity analyses (including as far as possible effects of a priory assumptions) and giving results with a reasonable range. I am fully aware that it would be hardly possible to do a full uncertainty analysis and even an sensitivity analysis might be quite ambitious given the catchment size and the complexity of the involved models. However, it is not enough just stating in the discussion some important processes are not taken into account.

Answer: We agree that an uncertainty analysis is important for a regional modelling study such as ours. Therefore, we performed additional simulations with a minimum and maximum soil erosion scenario, based on the uncertainty ranges in the rainfall erosivity and land cover factors of the Adjusted RUSLE model. Chapter 3 of the revised manuscript is modified to include the new uncertainty results. We also modified figure 9, which is figure 8 in the revised manuscript, to include the uncertainty ranges in the C budget components.

Regarding the sensitivity analysis of the model we tested the assumption of C enrichment during erosion as suggested by the reviewer. Here, we performed two additional simulations with an enrichment factor of two adapted from the study of Lugato et al. (2018): S1_EF (erosion only) and S2_EF (erosion with deposition and transport). We also tested the rate of C transport between floodplains by letting the basin average sediment residence time to vary between a 50% lower and 50% higher value compared to the default. For this purpose we did another two additional simulations (S2_Tmin and S2_Tmax). We also tested the model sensitivity to the crop residue management (S0_RM, S1_RM, S2_RM) as suggested by reviewer 1. Here we assumed an extreme scenario where all above-ground crop litter is harvested.

However, we abstained from testing the model performance to a changed C turnover in alluvial soils as a result of wetter conditions. Previous studies show that there are still large uncertainties related to the turnover of C in depositional environments, and more specifically of alluvial soils, as they represent complex soil profiles with a wide range in physical, chemical and biological parameters that affect the C turnover in interaction with climatic variables such as soil moisture. For example, the studies of Doetterl et al. (2018) and Rasmussen et al. (2018) show that the C turnover of alluvial soils is determined by C stabilization affected by the availability of minerals

(such as Iron, Aluminium) and nutrients, mediated by soil microbes and by the formation of peat deposits on river banks. Yet, old alluvial soils can be far from water-saturated, in which case the C turnover would not be substantially decreased as a result of additional oxygen limitation. In our study we also include floodplains that do not get flooded regularly. Therefore, it is not clear if these alluvial soils are in general 'wetter' than the colluvial soils and would therefore have a significantly different C turnover. Also, our model does not include a good representation of groundwater dynamics and a soil moisture function for alluvial soils. After performing an extensive literature study on C turnover in alluvial soils we could not find a way to easily but realistically modify the C turnover of alluvial soils, for example by using a simple turnover reduction factor derived from observations. We introduced a new section 4.3 in chapter 4, where we discuss the results from the sensitivity simulations. See changes to manuscript below.

Changes to manuscript: Section 2.11 lines 445-457, equation 15, and section 4.3 of the revised manuscript. See also the new tables 2 and 7, and adjusted figure 8 of the revised manuscript.

Comment 3: *From my understanding of the paper and accounting for the scope of the journal testing such new model against data is essential. The authors did try doing so but here a lot of improvement is easily possible: (i) Include a section under methods explain which data are used to test the model and also explain in some detail how this is done. For example, the comparison with other models as given in Fig. 3 and 5 is not clear, as the following information is missing: (a) Were the data from the more high resolution models aggregated to the raster cell size of CE-DYNAM to do a raster-by-raster comparison? (b) If a CE-DYNAM raster cell consist of erosional and depositional sites, which are not resolved in the raster cell, how to compare with gross erosion of a high resolution model (e.g. Panagos et al. 2015) which might have different proportions of erosional and depositional raster cells in this large 8 x 8 km 2 raster cell. (c) It is not clear at all what is compared as all model results from literature do not focus on the time span from 1850 to 2005. These details are essential for the reader to understand your model validation. (ii) From the figures I have some doubts that the different models fit very well (why not giving statistical goodness-of-fit-parameters?). So the question is how good the other models*

are (please see e.g. the scientific debate regarding the Panagos et al. (2015) map. So, at least in the discussion this model to model comparison needs to be stressed. (iii) Generally, the erosion (partly deposition) validation of CE-DYNAM is mostly done against other models also using USLE technology (USLE factors might be even derived from same data sources), so an extended discussion if this is meaning full is needed.

Answer: To better clarify the model validation and comparison against data and other models, included an additional section 2.12 in the revised manuscript where we discuss the validation data used, and how the validation is done in more detail. In this new section we also mention the reasons why we do this model to model comparison, where we provide more background information on the various models. Finally, we provide a statistical goodness-of-fit summary by comparing the total soil erosion and carbon erosion rates at sub-basin level to those of the other studies (see tables 3 and 4 of the revised manuscript).

Changes to manuscript: New section 2.12 on validation data and methods added to the revised manuscript. See also the new tables 3 and 4 of the revised manuscript.

Specific comments:

Comment S1: *Line 68-83: see general comment.*

Answer: See our response to general comment 1

Comment S2: *Line 89: be more explicit regarding 'low number of parameters'*

Changes to manuscript: See line 100-101 of the revised manuscript.

Comment S3: *Line 118 ff: I do not agree that not taking the L factor into account is a reasonable decision. I agree that it is somewhat difficult to estimate (for the German part of the Rhine catchment there are some estimates) but if you are interested in land use change it is an essential factor if you kick it out the entire basis of the USLE is set into question. (The P factor is simpler as it is set to 1 in most studies).*

Answer: We agree that leaving both the L and P factors out of the equation will induce some bias in the results, especially for agricultural land. In our next study we aim to make CE-DYNAM better applicable for agricultural land, where these factors play an important role. For this purpose we will focus on the development of new methods that can quantify the L and P factors reliably at the global scale, and will need to re-calibrate the erosion module of CE-DYNAM, the Adj.RUSLE. Our decision of leaving out the L and P factors from the erosion equation in our study is based on the global study of Doetterl et al. (2012), which showed that the S, R, C and K factors explain approximately 78% of the total erosion rates on cropland in the USA. This indicates that on cropland the L and P factors, which are related to agriculture and land management, contribute only for 22 % to the overall erosion rates. This percentage is comparable to the uncertainty range in the estimation of the S, R, C and K factors at the regional scale from coarse resolution data. Renard and Ferreira (1993) also mention that the soil loss estimates are less sensitive to slope length than to most other factors.

Furthermore, various studies argue that the estimation of the L factor for large areas is complicated and thus can induce significant uncertainty in soil erosion rates calculated based on coarse resolution data (Foster et al., RUSLE2 user guide; Kinnell, 2007). Especially, for natural landscapes, such as forest, the estimation of the L factor is not straightforward as these natural landscapes usually include steep slopes (Elliot, 2004). In order to stay consistent with the estimation of potential soil erosion for all land cover types, we remove the L factor from the equation. The Adj.RUSLE has been already successfully validated at the regional scale, without the L and P factors where the spatial variability of soil erosion rates compares well to other high resolution modeling studies and observational data and the absolute values fall within the uncertainty ranges of those validation data (Naipal et al., 2015; Naipal et al., 2016; Naipal et al., 2018; and this study). Finally, the aim of this study was to develop and validate a carbon erosion module for applications at the global scale, where the estimations of the L and P factors is even more limited. By showing that the erosion rates from the Adj.RUSLE and CE-DYNAM are within the uncertainty of other data and modelling studies, we can assume that it will be applicable for other large catchments in the temperate region.

Changes to manuscript: In section 4.2 'Model limitations' of the revised manuscript, we addressed the lack of the L and P factors in more detail in the same way as described above (see lines 750-771).

Comment S4: *Line 130: The statement ". . .has been calibrated and validated for the Rhine catchment. . ." is confusing here? If calibration and validation was already done why doing it again? If the model has changed you need a new validation (but what about calibration? Are you using parameters in CE-DYNAM which were calibrated before it is necessary to indicate this in detail).*

Answer: In our study we use the model parameters of the global sediment budget model as defined and calibrated by Naipal et al. (2016), such as the sediment residence time or the floodplain deposition factor. We did not perform an additional calibration of the sediment dynamics part of CE-DYNAM, only a validation, because of the use of different input datasets.

Changes to manuscript: We added a sentence specifying why we redid the validation, see line 467-468 of section 2.12 in the revised manuscript.

Comment S5: *Line 113: Alluvial soils are indicated in German soil maps, so the statement is not correct for the largest part of the Rhine catchment.*

Changes to manuscript: We will modify the sentence to: 'It should be noted that global soil databases do not identify floodplain soil as a separate soil class, although national soil databases might. However, the aim of this study is to present a carbon erosion model that should be also applicable for other catchments and eventually, globally. Therefore, we followed a 2-step methodology to derive floodplains in the Rhine catchment using hydrological parameters and existing data on hillslopes and valleys.' See lines 151-155 of section 2.3 of the revised manuscript.

Comment S6: *Line 141 / Eq. 2: Generally I think it would be good being more precise with the equation. For example in case of Eq. 2, I would expect a reference to the different raster cells*

(Aft(i) = Lstream(i) x Wstream(i); whereas i is the raster cell.) as for other equations e.g. Eq. 4a it was not clear if this refers to the entire catchment is calculated for each raster cell.

Changes to manuscript: We modified the equations accordingly in the revised manuscript.

Comment S7: *Line 148: If alpha and b are constants it means that the upstream area necessary to result in a stream is always the same. I understand that in case of a large scale model simplifications are necessary but this assumptions is for sure not true for the Rhine catchment (see papers from hydrology of maps of the stream system (which by the way would be available for the entire Rhine catchment).*

Answer: We agree, that they might not be the same for the entire catchment, and variations exist. But these constants have been derived from 467 cross-sections of the Rhine catchment combining 1:25 000 geological maps and catchment area extracted from the SRTM 3 arcsec digital elevation model (Hoffmann et al., 2007).

Comment S8: *Line 159: '. . . at 8 km resolution. . . " I guess this means 8 km x 8 km raster cells. Should be changed throughout the text (also with other resolution given).*

Answer: Yes, this means indeed a 8 km x 8 km raster. We added a sentence in section 2.3 explaining this.

Changes to manuscript: See line 138-140 of section 2.2

Comment S9: *Line 163: I do not think the the assumptions of reduced hydrological and geomorphological connectivity in arable landscapes (compared to forest) is correct. From the recent studies dealing with flash floods it is obvious that it is a main problem that this landscapes have a very high connectivity as so many ditches, drainages etc. were built over the last century to get rid of any surplus of water on arable land. So, your assumptions for the range of the parameter f in different landscapes must be underlined by reasonable data.*

Answer: This assumption is underlied by several studies (Hoffmann et al., 2013; de Moor and Verstraeten, 2008; Gumiere et al., 2011;Wang et al., 2015) on the effect of erosion on sediment

yield, where is shown that man-made activities on agricultural landscapes result in a trapping of eroded soil in colluvial deposition sites, reducing the sediment transport from hillslopes to the floodplains. The model parameter *f* has been calibrated for the Rhine catchment before in Naipal et al. (2016), where this range is found to produce a ratio between hillslope and floodplain sediment storage that was comparable to observations. The studies of Wang et al. (2010; 2015) identify a range for the hillslope sediment delivery to be between 50 and 80 %, which is similar to the range in the (1-f) factor of our model.

Changes to manuscript: We included these arguments on the choice for the *f* parameter in section 2.3 lines 188-196 of the revised manuscript.

Comment S10: *Line 187: Does a multiple flow algorithm makes sense in case of a resolution of 8 km*

Answer: The multiple flow algorithm is especially effective in hilly regions, and we expect it to work better than the single flow algorithm for these regions. In such steep landscapes the river courses are meandering a lot. So the downstream part of a river can easily cut through the boundary of two downstream lying adjacent 8 km x 8 km cells. With the coarse resolution of 8 km, a single direction algorithm would lead to an extreme straightening of the river network, and it would underestimate the number of cells which have a proportion of floodplain area. However, we agree that the coarse resolution grid size will affect the results of both algorithms.

Comment S11: *Line 230 ff: In general this is a reasonable assumption for the crop residues. However, studies in small catchment clearly indicate that residue management is a key factor of SOC, so this a priori assumption has potentially a huge effect on the produced results. So, its importance must be analyzed with the model!*

Answer: We agree that the harvest and crop residues left on the field would have a large effect on the SOC dynamics of agricultural landscapes. It should be noted that we implemented an increase in the harvest index during the period 1850-present-day based on the study of Hay (1995), which already partly accounts for crop residue management. To explicitly quantify the

potential impacts of crop residue management we performed additional sensitivity simulations where we assumed that all above-ground crop residues are harvested. After running CE-DYNAM with crop residue management we find that total litter C stock is about 15% smaller compared to the default case by the end of the year 2005. This leads to a total change in the transient SOC stocks that is 20% smaller under no erosion (S0), and 26% smaller under erosion (S2). Our findings confirm that soil management practices such as residue management have a substantial effect on the SOC dynamics.

Changes to manuscript: Section 2.11 and table 2 of the revised manuscript describes the setup of the sensitivity simulations with respect to crop residue management. The new section 4.3 and table 7 present the results of crop residue management.

Comment S12: *Line 238-240: The given equation are a fundamental problem with modelling the effect of soil erosion on SOC turnover. For example, using standard SOC pool residence times for all landscape positions is of tremendous importance for the entire C balance effect of erosion. So, again it would be very important to know how sensitive the results are against this assumptions. At least give some estimates / measurements at different landscape positions in the discussion and comment of the potential effect in modelling results.*

Answer: The SOC pool residence times at different landscape positions (hillslope, depositional sites etc), is interrelated with weathering, soil erosion and sediment transport processes (Berhe et al., 2008). To be able to have different residence times for each SOC pool as a function of the landscape position, soil erosion effects on for example the aggregation of soil particles and transport of minerals and nutrients has to be included. This can currently not be done in global land surface models. However, there are efforts to change the current SOC dynamics scheme of LSMs by introducing measurable SOC pools (Abramoff et al., 2018). In this case it might be possible to calibrate the residence time of each pool based on the landscape position.

Changes to manuscript: See lines 739-743 in section 4.2 of the revised manuscript.

Comment S13: *Line 265: ". . . The next soil layer contains less C and therefore at the following time-step les C will be eroded under the same erosion rate. . ." If this would be always true one would expect a continuous decline in SOC in soils. However, assuming a long- term forest use on a slope you will found the soil in an equilibrium between new C input via plants and small amount of erosion. So, in this case the eroded material will have a more or less constant C content.*

Answer: We understand that this sentence might be unclear. What we mean is that the reduction of C erosion at each timestep due to less C being available for erosion, and the existence of a compensatory C sink due to the erosional removal of C, will ultimately lead to an equilibrium state. Which is also reached in our model.

Changes to manuscript: We add the following sentences to the revised manuscript (lines 308-310 of section 2.7): " The removal of C by erosion also triggers a compensatory C sink due to the reduction in SOC respiration on eroding land. This compensatory C sink and reduced C erosion over time will ultimately lead to an equilibrium state."

Comment S14: *Line 277: Calculating a daily erosion fraction is a reasonable approach. However, if taking the episodic nature of erosion and deposition into account the C balance will be different compared to a small continuous process (see literature). Might be also discussed.*

Answer: We will mention this aspect in the discussion chapter of the revised manuscript.

Changes to manuscript: See lines 773-776 of section 4.3 of the revised manuscript.

Comment S15: *Line 291 ff: The assumption that there is no C selectivity (enrichment in eroded material and depletion at erosional sites) is taken in many modelling approaches. However, if there would be no enrichment of fines in the sediments transported in river systems, one would find e.g. sand in suspended sediments of larger rivers. Which is e.g. in case of the lowland Rhine not the case. Discuss this in the context of the scale of your paper. Also important regarding the loss of C to the ocean.*

Answer: We agree and performed a sensitivity analysis of the model where we changed the C enrichment factor to 2 , hereby, partly accounting for the selectivity of erosion. We find that although the POC export to the ocean is not significantly affected, the SOC storage and resulting C sink is increased. See our detailed response to general comment 2.

Comment S16: *Line 341: Where do the data regarding afforestation during the last two decades come from. To my knowledge this is a process already started in the late 1959th (please give reference)*

Answer: We use the land use change data from the study of Peng et al. (2017), who bases their estimates of forest cover on Houghton (2003,2008) for the period 1850-1990 and satellite data for the recent decades. The historical national forest area used by Houghton et al. since 1850 are from national surveys and they are arguably the best data available, although uncertainty arises when downscaling historical forest area change on a grid, using (uncertain) gridded reconstruction of agricultural land (HYDE) and land use transitions rules (see details for the method used by Peng et al. 2017).

Comment S17: *Line 379: (see also general comments). I wonder why you did not use other more specific and potentially profound national data. E.g. for Germany there are several maps for potential erosion which are much more elaborated than the map of Panagos et al. (2015). Moreover, I wonder why you did not use the sediment delivery data of the Rhine which are freely available - I guess since the 1950th - which would be a good and reliable additional data set for validation.*

Answer: We did not use the sediment delivery data of the Rhine, because the comparison to our simulated coarse resolution model results will most likely be not entirely justified. In our model we do not take into account daily changes in precipitation and runoff and how that affects the erosion rates and sediment transport. Instead we use yearly totals. We also do not take into account dams and other man-made structures that would affect the river transport of sediment. Further, we focus only on the rill and interrill erosion and do not account for other soil erosion

processes and flash floods that might have a larger effect on the sediment delivery. Finally, our model has not been developed to simulate the river transport of sediment and C, but instead is focused on the redistribution of soil on land and the resulting sediment and SOC storage. See also our response to the general comment of reviewer 1. For the future development of CE-DYNAM we aim to better represent the river transport processes of sediment and C.

Regarding the validation of soil erosion with observations, we used the database of Cerdan et al. (2010), which already includes German national estimates on soil erosion. We also performed a comparison of our agricultural soil erosion model estimates to the agricultural soil erosion potential map of the Federal Institute for Geosciences and Natural Resources of Germany, available at 250 m resolution, in the revised manuscript.

Changes to manuscript: Figure 3C is added and discussed in section 3.1 of the revised manuscript. Section 2.12 describes the German soil erosion map used for validation.

Comment S18: *Line 397-401: I suggest omitting these sentences and Fig. 4, because I do not see any additional value of this here. It is obvious from the model structure of all USLE based models (and all other erosion models) that an increase of erosivity and slope directly leads to an increase in erosion. Moreover, there is a coincidence in the catchment that highest erosivity and highest slopes occur at the same alpine area, but this is not any proof for the model. Hence, hence I think this is weakening your validation more that it would strengthen it. By the way: Erosivity and slope might explain 70% erosion if very different rainfall regimes and slopes (mountain areas and lowlands) are compared, but with a catchment like the Rhine (where except for the alpine part) the differences in slope and erosivity are relatively small soil cover (C factor) is getting much more important (erosion rates between grassland and arable land vary by a factor of 10-20).*

Answer: We agree and omitted figure 4 in the revised manuscript.

Comment S19: *Line 402: As I modeler I expect a goodness-of-fit parameter with this statement. (See also general comments regarding model to model comparison of different USLE implementations).*

Answer: We included a goodness-of-fit summary related to the soil erosion result comparison at sub-basin level, see our response to comment 3.

Changes to manuscript: See new table 3 and 4 of the revised manuscript and their description in section 3.1

Comment S20: *Line 424 ff: The comparison with the data from Hoffman et al. (2013) underlines a deficit in all your comparisons. It is at no time clear what is compared exactly. Mean of 7500 years against 1850-2005?*

Answer: See the last paragraph in our response to general comment 3 and modifications to the manuscript.

Comment S21: *Line 438: Does the outflux fit to measured data? Would be easy to test even if this is not essential as only a very small amount will be delivered into the sea. (could be tested at several subcatchment, as data are available).*

Answer: See our response to general comment 1 of reviewer 1

Changes to manuscript: See lines 703-724 of section 4.2 of the revised manuscript.

Comment S22: *Line 451-452: This is a clear contradiction to your statement that differences in erosivity are very important for spatial differences in erosion.*

Answer: We agree and removed this sentence in the revised manuscript.

Comment S23: *Line 453: The close link between C erosion and soil erosion is obvious from your modelling structure but not necessarily correct (C enrichment depending on event size?)*

Changes to manuscript: See lines 592-594 of section 3.2 of revised manuscript

Comment S24: *Line 434 ff: See also general comments*

Answer: We address this in our response to the general comments

Comment S25: *Line 446: I suggest not to over interpret the modeling results from the alpine area of the catchment as the modelling and the data are weakest there. (i) Increase in measured precipitation most uncertain; (ii) calculated R factor very uncertain in all USLE approaches; (iii) alpine USLE factors not very well underlined by data (compared to arable and grassland),*

Answer: We agree and are aware of this bias and therefore, present all model and validation results for the non-alpine region only.

Changes to manuscript: See line 534-535 at the beginning of chapter 3 of the revised manuscript.

Comment S26: *Line 497ff. See comments regarding connectivity above. Moreover, even if the connectivity is high under forest (which I doubt), forest will produce not a lot of sediment and hence are not so important for building up alluvial soils at all.*

Answer: We agree that soil erosion in forests is minimal but forests also appear often in hilly landscapes that will contribute to the sediment production. When analyzing soil erosion rates over timescales longer than a few decades, extensive forest areas will contribute significantly to the overall removal of soil. Forests contain also a lot of SOC, and so minimal rates of soil erosion might be still significant for the SOC dynamics, also in depositional areas, as is demonstrated in the recent study of Billings et al. (2019).

Comment S27: *Line 493ff. I do not see from the results the CO2 fertilization plays an important role for an increase in dynamic replacement. I guess that the increase in yields due to changes in management are much more important (as reduced yields are not taken into account at erosional sites) as they boost dynamic replacement of eroded soils.*

Answer: We agree that increased yields due to management boost the dynamic replacement of eroded soil but the largest effect comes from the CO_2 fertilization due to increased atm. CO_2

concentrations. See below figure 1 representing the actual C replacement under land use change and climate change, and figure 2 representing the potential C replacement under a fixed climate (no change in temperature, precipitation, CO2 atm. concentrations, but with a changing land use and management).

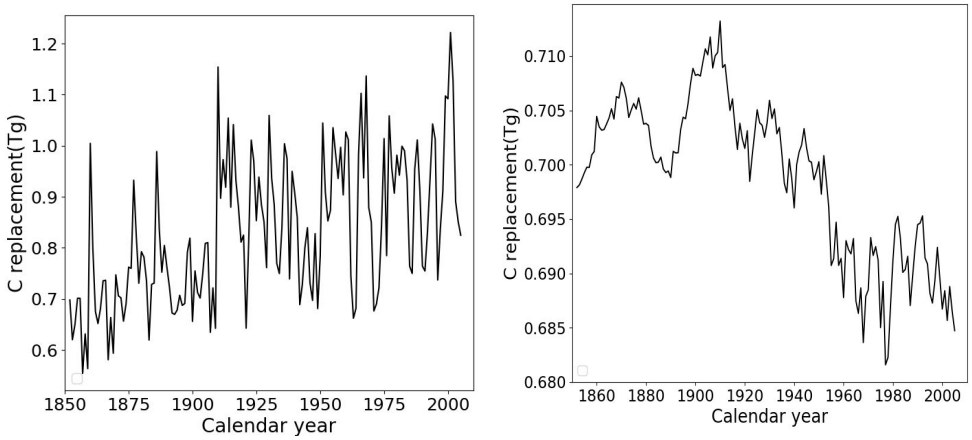

Fig 1 & 2: C replacement on eroding soils

Changes to manuscript: We include these figures in the supplementary material section S4 A&B

Comment S28: *Line 501ff: It is obvious from first order kinetics that colluvial soils must have higher CO2 effluxes as they contain more C. So, this is not a very new finding.*

Answer: We agree that this might be an obvious finding, but this has not been quantified for such a large catchment before. With this finding we also indicate that the model reproduces process knowledge from field work.

Comment S29: *Line 506-507: Question: Is the modelled increase in respiration from floodplains resulting from an temperature increase or from an increase in depositional material, which would also result in an increase of respiration? Comment: Under real conditions the increase in respiration from floodplains is also a result of decreasing groundwater levels,*

Answer: After redoing the simulations using a better spinup method (see section 2.11, lines 436-439) we find that the respiration from floodplains is rather variable and shows a decreasing

trend. This is mainly a result of a decreased C deposition flux. In our model we do not have a specific representation of ground water for floodplains.

Changes to manuscript: See lines 644-653 of section 3.2 of the revised manuscript

Comment S30: *Line 542-561: This is a nice collection of model deficits. However, for a modelling paper I would expect a bit more (see general comments).*

Answer: See our response to the general comments and resulting improvements made to the manuscript.

Comment S31: *Line 576-588: I think this conclusions are not fully supported by the results as the modelled C fluxes might be affected by a priori assumptions and model parameters which are not tested enough (see general comment regarding sensitivity analysis).*

Answer: We adjusted the findings in the conclusions

Changes to manuscript: See lines 836-839 of chapter 5 of the revised manuscript and lines 845-846.

Comment S32: *Table 1: I guess the spatial resolution is always given in raster cells, e.g. 0.25 ◦ x 0.25 ◦*

Answer: See our response to comment S10 and respective changes in the revised manuscript.

Comment S33: *Table 2: As the resolution of the data sets are different how to make sure that the comparison fits, e.g. the higher resolution data set might exclude the river network from the SOC calculation while the lower resolution data set might include this areas into the SOC stock calculation. Give somewhat more details.*

Answer: We give more details on the resolution and comparison in the new section 2.12 of the revised manuscript. See our response to comment 3.

Comment S34: *Fig. 3 and 5: What are the 10 classes given on the X-Axis?*

Answer: The x-axis represents bins or evenly spaced ranges between the minimum and maximum erosion or deposition rates. We adjusted the figure caption to include this information in the revised manuscript.

Comment S35: *Fig. 4. Omit this figure (see comment above)*
Answer: Is removed

Comment S36: *Fig. 5c/d: What does it mean if CE-DYNAM has erosion rates which are up to a factor smaller than the Lugato model and C deposition rates which are more or less the same? Is it a result of different areas affected by erosion and deposition? Should be explained / discussed.*
Answer: This was a mistake as we used different bins on the x-axis for the different datasets. after changing the ranges for the bins we find that the simulated rates and those of Lugato et al. are similar. Thank you for pointing this out.
Changes to manuscript: See the new figure 4c/d of the revised manuscript

Comment S37: *Fig. 7. Just a comment of an handicapped. About 4-8% of the male population are to a certain extend color blind (especially red/green is problematic), so if you do not what to lose these proportion of your readers you should adapted your color in your figures. There are color blind friendly color ranges available in most software packages. If the dashed lines range between min and max the outliers cannot be above or below the lines. So, I guess the lines represent something else.*
Answer: We apologize for this oversight and used patterns and different line styles to adapt figures 5, 6 and 7 of the revised manuscript, where we expect difficulties for color-blind readers. The dashed lines in figure 7 do not represent the min and max but the outer extremes. The outliers are defined as values that are larger than the 3th quantile by at least 1.5 times the interquartile range (IQR), or smaller than 1st quantile by at least 1.5 times the IQR.
Changes to manuscript: See the adapted new figure 5,6 and 7

CE-DYNAM (v1), a spatially explicit, process-based carbon erosion scheme for the use in Earth system models

Victoria Naipal[1,2], Ronny Lauerwald[32], Philippe Ciais[21], Bertrand Guenet[21], Yilong Wang[21]

[1] Ludwig-Maximilians University, Munich, Germany

[21]Laboratoire des Sciences des Sciences du Climat et de l'Environnement, CEA CNRS UVSQ, Gif-sur-Yvette 91191, France

[32]Department of Geoscience, Environment and Society, Université Libre de Bruxelles, Brussels, Belgium

Correspondence : Victoria Naipal (vnaipal24@gmail.com)

Abstract. Soil erosion by rainfall and runoff is an important process behind the redistribution of soil organic carbon (SOC) over land, hereby impacting the exchange of carbon (C) between land, atmosphere and rivers. However, the net role of soil erosion in the global C cycle is still unclear as it involves small-scale SOC removal, transport and re-deposition processes that can only be addressed over selected small regions with measurements and models. This leads to uncertainties in future projections of SOC stocks and complicates the evaluation of strategies to mitigate climate change through increased SOC sequestration.

In this study we present the parsimonious process-based Carbon Erosion DYNAMics model (CE-DYNAM) that links sediment dynamics resulting from water erosion with the C cycle along a cascade of hillslopes, floodplains and rivers. The model simulates horizontal soil and C transfers triggered by erosion across landscapes and the resulting changes in land-atmosphere CO_2 fluxes at a resolution of about 8 km at the catchment scale. CE-DYNAM is the result of the coupling of a previously developed coarse-resolution sediment budget model and the ecosystem C cycle and erosion removal model derived from the ORCHIDEE land surface model. CE-DYNAM is driven by spatially explicit historical land use change, climate forcing, and global atmospheric CO_2 concentrations affecting ecosystem productivity, erosion rates and residence times of sediment and C in deposition sites. The main features of CE-DYNAM are (1) the spatially explicit simulation of sediment and C fluxes linking hillslopes and floodplains, (2) the relative low number of parameters that allow running the model at large spatial scales and over long-time scales, and (3) its compatibility with ~~any~~ global land surface models, hereby, providing opportunities to study the effect of soil erosion under global changes.

We present the model structure, concepts, and evaluation at the scale of the Rhine catchment for the period 1850-2005 AD. Model results are validated against independent estimates of gross and net soil and C erosion rates, and the spatial variability of SOC stocks from high-resolution modeling studies and observational datasets**.** We show that despite local differences, the resulting soil and C erosion rates, and SOC stocks from CE-DYNAM ~~our rather coarse-resolution~~

modelling approach are comparable to high-resolution estimates and observations at sub-basin level. The model also shows that SOC storage increases exponentially with basin area for floodplains in contrast to hillslopes as is seen in observations.

We find that soil erosion mobilized around 66±28159 Tg (10^{12} g) of C under changing climate and land use over the non-Alpine region of the Rhine catchment, assuming that the erosion loop of the C cycle was in near steady-state by 1850. This caused a net C sink equal to 2.1-2.71% of the Net Primary Productivity of the non-Alpine regionRhine catchment over 1850-2005 AD. This sink is a result of the dynamic replacement of C on eroding sites that increases in this period due to rising atmospheric CO_2 concentrations enhancing the litter C input to the soil from primary production.

Keywords. soil erosion; regional carbon cycle; carbon sink; Rhine catchment; regional modelling

1 Introduction

Soils contain more carbon (C) than the atmosphere and living biomass together. Relatively small disturbances (anthropogenic or natural) to soil C pools over large areas could add up to substantial C emissions (Ciais et al., 2013). With the removal of natural vegetation and the introduction of mechanized agriculture, humans have accelerated soil erosion rates. Over the last two to three decades, studies have shown that water erosion (soil erosion by rainfall and runoff) amplified by human activities has substantially impacted the terrestrial C budget (Doetterl et al., 2012; Lal, 2003; Lugato et al., 2018; Van Oost et al., 2007, 2012; Stallard, 1998; Wang et al., 2017). However, the net effect of water erosion on the C cycle at regional to global scale is still under debate. This leads to uncertainties in the future projections of the soil organic C (SOC) reservoir, and complicates the evaluation of strategies to mitigate climate change by increased SOC sequestration. The study of Stallard (1998) was one of the first to show that water erosion does not only lead to additional C emissions but can also sequester C due to the photosynthetic replacement of SOC at eroding sites and the stabilization of SOC in deeper layers at burial sites. The study of van Oost et al. (2007) was the first to confirm the importance of the sequestration of SOC by agricultural erosion at global scale using isotope tracers. Wang et al. (2017) gathered data on SOC profiles from erosion and deposition sites and confirmed that water erosion on agricultural land that started from the early/middle Holocene has caused a large net global land C sink. Other studies, however, argue that soil erosion is a net C source to the atmosphere due to increased SOC decomposition following soil aggregate breakdown during transport and at deposition sites (Lal et al, 2003; Lugato et al., 2018). Most studies modeling soil erosion and its net effect on SOC dynamics at global scale, however, did not account for the full range of complex effects of climate change, CO_2 fertilization increasing productivity and potentially soil C inputs, harvest of biomass, land use change, and changes in cropland management. In addition, models used at large spatial scales mainly focus on hillslopes and removal processes and neglect floodplain sediment and SOC dynamics. This can lead to substantial biases in the assessment of net effects of SOC erosion at catchment scale because floodplains can store substantial amounts of sediment and C (Berhe et al., 2007; Hoffmann et al.,

2013a). Studies addressing long-term large-scale sediment yield from hillslopes and floodplains, such as Pelletier et al. (2012), do not explicitly account for the redistribution of sediment and SOC over land.

Furthermore, soil erosion is one of the main contributors to particulate organic carbon (POC) fluxes in rivers and C export to the coastal ocean. The riverine POC fluxes are usually much smaller than the SOC erosion fluxes, because only a small fraction of eroded material is entering the river network, while ~~and~~ POC losses occur in the river network and ~~occur~~ due to decomposition and burial ~~i~~on floodplains and in benthic sediments (Tan et al., 2017; Galy et al., 2015). Therefore, uncertainties in large-scale SOC erosion rates will lead to even larger uncertainties in lateral C fluxes between land and ocean for past and future scenarios estimated by global empirical models on riverine C export (Ludwig and Probst, 1998; Mayorga et al., 2010).

To address these knowledge gaps, we present a parsimonious process-based Carbon Erosion Dynamics Model (CE-DYNAM), which integrates sediment dynamics resulting from water erosion with the SOC dynamics at the regional scale. The SOC dynamics are calculated consistently with drivers of land use change, CO_2 and climate change by a process-based land surface model (LSM), with a simplified reconstruction of the last century increase of crop productivity. This modelling approach consists of a global sediment budget model coupled to the SOC removal, input, and decomposition processes diagnosed from the ORCHIDEE global LSM in an offline setting (Naipal et al., 2018). The main aim of our study is to quantify the horizontal transport of sediment and C along the continuum of hillslopes, floodplains and rivers, and at the same time analyze its impacts on the land-atmosphere C exchange. We validate the new model with regional observations and high-resolution modelling results of the Rhine catchment. It should be noted here that the structure of CE-DYNAM is designed in a way that the model can be adapted easily to other large catchments and finally run globally. We also discuss the model uncertainties and the sensitivity of the model to changes in key model parameters and assumptions made. In the next sections we give a detailed overview of CE-DYNAM model structure, the coupling of erosion, deposition and transport with the coarse-resolution SOC dynamics of ORCHIDEE, model application and validation for the non-Alpine region of the Rhine catchment, and its potentials and limitations.

~~To address these knowledge gaps, we present a parsimonious process-based modelling approach that integrates sediment dynamics resulting from water erosion with SOC dynamics and the horizontal transport of sediment and C in the continuum from hillslopes, to floodplains and rivers. With this approach we are not only able to simulate lateral soil and C transfers triggered by erosion across landscapes but also the resulting changes in the land-atmosphere CO_2 fluxes. The modelling approach uses a simple sediment budget model which is coupled to SOC erosion removal, C input from litter fall, and SOC decomposition processes diagnosed from the ORCHIDEE global land surface model (LSM) in an offline setting (Naipal et al., 2018). We parameterized and applied the resulting model, known as CE-DYNAM for the Rhine catchment, although it is intended to be made applicable to other large catchments globally. CE-DYNAM combines soil erosion processes, for which small scale differences in topography are of utter importance, with a state-of-the-art representation of large-scale SOC dynamics driven by land use and environmental factors (climate, atmospheric CO_2) as simulated by the ORCHIDEE LSM. The flexible structure of CE-DYNAM makes the model adaptable to the SOC~~

dynamics of any other LSM. In this way it is possible to study the main processes behind the linkages between soil erosion and the global C cycle. ¶

¶

In the next sections we give a detailed overview of CE-DYNAM model structure, the coupling of erosion, deposition and transport with the coarse-resolution SOC dynamics of ORCHIDEE. We then discuss its application for the Rhine catchment, model limitations, uncertainties and its potentials.¶

2 Methods

2.1 General model description

CE-DYNAM version 1 (v1) is the result of coupling a large-scale erosion and sediment budget model (Naipal et al., 2016) with the SOC scheme of the land surface model ORCHIDEE (Krinner et al., 2005). The most important features of the model are (1) the spatially explicit simulation of lateral sediment and C transport fluxes over land linking hillslopes and floodplains, (2) consistent simulation of vertical C fluxes coupled with horizontal transport, (3) the low number of parameters that allows running the model at large spatial scales and over ~~long~~ time-scales up to several thousands of years, (4) the generic input fields for application to any region or catchment, and (5) compatibility with land surface models (LSMs).

In the ORCHIDEE LSM, terrestrial C is represented by eight~~8~~ biomass pools, four~~4~~ litter pools and three~~3~~ SOC pools. Each of the pools varies in space, time and over the twelve ~~12~~ Plant Functional Types (PFTs). An extra PFT is used to represent bare soil. Natural and anthropogenic disturbances to the C pools include fire, crop harvest, changes to GPP, litterfall, autotrophic and heterotrophic respiration as a result of climatic changes (Krinner et al., 2005; Guimberteau et al., 2018). The C-cycle processes are represented by a C emulator that reproduces for each PFT all C pools and fluxes between the pools exactly as in ORCHIDEE in absence of erosion. A net land use change scheme is included in the emulator with mass-conservative bookkeeping of SOC and C input when a PFT is changed into another from anthropogenic land use change (Naipal et al., 2018). The sediment budget model has been added in the emulator to simulate large-scale long-term soil and SOC redistribution by water erosion using coarse-resolution precipitation, land-cover and LAI data from Earth System Models (Naipal et al. 2015, 2016). The C emulator including erosion removal was developed by Naipal et al. (2018) to reproduce SOC vertical profile, removal of soil and SOC starting from the topsoil, and compensatory SOC storage from litter input. As soil erosion is assumed not to change soil and hydraulic parameters but only the SOC dynamics, the emulator allows substituting for the ORCHIDEE model and performing simulations on time scales of millennia with a daily time step, which would be a very computationally expensive or nearly impossible with the full LSM. The concept and all equations of the emulator are described in Naipal et al. (2018). The following subsections describe the

different components of the CE-DYNAM that couples the C and soil removal scheme (Naipal et al., 2018) with the horizontal transport and burial of eroded soil and C (Naipal et al., 2016).

2.2 The soil erosion scheme

The potential gross soil erosion rates are calculated by the Adjusted Revised Universal Soil Loss Equation (Adj. RUSLE) model (Naipal et al., 2015), which is part of the sediment budget model (Fig 1). In the Adj. RUSLE the yearly average soil erosion rate is a product of rainfall erosivity (*R*), slope steepness (*S*), land cover and management (*Cm*) and soil erodibility (*K*):

$$E = S * R * K * Cm \quad (1)$$

The slope-length (*L*) and support practice (*P*) factors, which are part of the original Revised Universal Soil Loss Equation (RUSLE) model (Renard et al., 1997), have been excluded here because their quantification still includes many uncertainties and is not practical for applications at regional to global scales. These factors are a function of local manmade structures and management practices which are difficult to assess for present day and whose changes over the past are even more uncertain. In addition, we focus in this study on potential soil erosion and do not consider erosion-control practices.
Naipal et al. (2015) have developed a methodology to derive the slope factor *S* and the erosivity factor *R* from 5 arcmin resolution (5 x 5 arcminute raster) data on elevation and precipitation, hereby preserving the high-resolution spatial variability in slope and temporal variability in erosivity. In the rest of the manuscript we will refer to X by X km/arcminute raster cells alway with X km/arcmin resolution. Despite the comparatively coarse resolution of the erosion model, the so derived *R* factor was shown to compare well with the corresponding high-resolution product published by Panagos et al. (2017). In the study of Naipal et al. (2016), where the soil erosion model was applied for the last millennium, the change in climate was taken into account in the calculation of the *R* factor. For this study, we assume that the climate zones as defined by the Koeppen-Geiger climate classification have not changed drastically since 1850 AD.

2.3 The sediment deposition and transport scheme

The sediment deposition and transport scheme have been adapted from the sediment budget model described by Naipal et al. (2016), which has been calibrated and validated for the Rhine catchment (Fig 1). In the sediment budget model each grid cell contains a floodplain fraction, which is needed to ensure sediment transport between the grid cells (transport from one grid cell to another can only follow the connectivity of floodplains). It should be noted that global soil databases do not identify floodplain soil as a separate soil class, although national soil databases might. However, the aim of this study is to present a carbon erosion model that should be also applicable for other catchments and eventually, globally. Therefore, we followed a two-step methodology to derive floodplains in the Rhine catchment using hydrological parameters and existing

data on hillslopes and valleys. ~~We followed a 2-step methodology to derive floodplains in the Rhine catchment, as soil databases usually do not identify floodplain soil as a separate soil class.~~ First, grid cells were identified that consisted entirely out of floodplains. For this we used the gridded global data set of soil at 5 arcminute resolution, with intact regolith, and sedimentary deposit thicknesses of Pelletier et al. (2016) (Table 1), and identified lowlands and hillslopes based on soil thickness and depth to bedrock. The lowlands were classified as grid cells that contain only floodplains and no hillslopes. Second, we calculated the floodplain fraction (A_{fl}) of a grid cell i ~~(A_{fl})~~ that has both hillslopes and floodplains as a function of stream length and width based on the methodology developed by Hoffmann et al. (2007):

$$A_{fl}(i) = L_{stream}(i) * W_{stream}(i) \quad (2)$$

Where, L_{stream} is the stream length derived from the HydroSHEDS database (Lehner and Grill, 2013) (Table 1).

$$W_{stream}(i) = a * A_{upstream}^{b}(i) \quad (3)$$

Where, $A_{upstream}$ is the upstream catchment area, and a is equal to 60.8, and b is equal to 0.3.

The parameters a and b have been derived from the scaling behavior of floodplain width as estimated from measurements on the Rhine (Hoffmann et al., 2007). The sediment deposition on hillslopes (D_{hs}) and floodplains (D_{fl}) is calculated as a function of the gross soil removal rates (E) according to Naipal et al. (2016) with the following equations:

$$D_{fl}(i) = f(i) * E(i) \quad (4a)$$

$$D_{hs}(i) = (1 - f(i)) * E(i) \quad (4b)$$

$$f(i) = a_f * e^{\left(\frac{b_f * \theta(i)}{\theta_{max}}\right)} \quad (5)$$

Where, f is the floodplain deposition factor at 8 km resolution that determines the fraction of gross eroded material transported and deposited in the floodplain fraction of a grid cell. a_f and b_f are constant parameters that relate f to the average topographical slope (θ) of a grid cell depending on the type of land cover . θ_{max} us the maximum topographical slope of the entire Rhine catchment.

The parameters a_f and b_f are chosen in such a way that f varies between 0.2 and 0.5 for cropland, reflecting the decreased sediment connectivity between hillslopes and floodplains created by man made~~manmade~~ structures such as ditches and hedges. For natural vegetation such as forests and natural grassland, a_f and b_f are chosen in a way that f varies between 0.5 and 0.8 assuming that in these landscapes hillslopes and floodplains are well-connected. This assumption on the reduced

sediment connectivity for agricultural landscapes is supported by several previous studies (Hoffmann et al., 2013; de Moor and Verstraeten, 2008; Gumiere et al., 2011;Wang et al., 2015) on the effect of erosion on sediment yield. These studies show that man-made activities on agricultural landscapes result in a trapping of eroded soil in colluvial deposition sites, reducing the sediment transport from hillslopes to floodplains. The model parameter *f* has been calibrated for the Rhine catchment before in Naipal et al. (2016), where the ranges mentioned above are found to produce a ratio between hillslope and floodplain sediment storage that was comparable to observations. The studies of Wang et al. (2010; 2015) identify a range for the hillslope sediment delivery to be between 50 and 80 %, which is similar to the range in the (1-f) factor in our model. In each case and within the defined boundaries, the slope gradient determines the final value of *f*. Eroded material that has not been deposited in the floodplains stays on the hillslopes and is assumed to be deposited at the foot of the hillslopes as colluvial sediment.

The floodplain fractions of the grid cells are connected through an 8 km resolution flow routing network (Naipal et al., 2016), where the rivers and streams are indirectly included in the floodplain area but not explicitly simulated. By routing the sediment and C through the floodplain fractions of grid cells we lump together the slow process of riverbank erosion by river dynamics (time scale ≈ a few years to thousands of years), and the rather fast process of transport of eroded material by the rivers (time scale ≈ days). The rate by which sediment and SOC leave the floodplain of a grid cell to go to the floodplain of an adjacent grid cell is determined by the sediment residence time. The sediment residence time (τ) is a function of the upstream contributing area (*Flowacc*):

$$\tau(i) = e^{\frac{Flowacc(i)-a_\tau}{b_\tau}} \quad (6)$$

The study of Hoffmann et al. (2008) shows that the majority of floodplain sediments have a residence time that ranges between 0 and 2000 years, with a median of 50 years. The constants a_τ and b_τ are chosen in such way that basin τ varies between the 5th and 95th percentile of those observations, with a median for the whole catchment of 50 years. These constants are uniform for the whole basin. Floodplain C storage follows the same residence time as sediment on top of the actual decomposition rate of C in a grid cell of ORCHIDEE. The routing of sediment and C between the grid cells follows a multiple-flow routing scheme. In this scheme the flow coming from a certain grid cell is distributed across all lower-lying neighbors based on a weight (*W*, dimensionless) that is calculated as a function of the contour length (*c*):

$$W_{(i+k,j+l)} = \frac{\theta_{(i+k,j+l)} * c_{(i+k,j+l)}}{\sum_{k,l=-1}^{k,l=1} \left[\theta_{(i+k,j+l)} * c_{(i+k,j+l)}\right]} \quad (7)$$

Where *c* is 0.5*grid size (m) in the cardinal direction and 0.354* grid size (m) in the diagonal direction. (*i, j*) is the grid cell in consideration where *i* counts grid cells in the latitude direction and *j* in the longitude direction. *i*+*k* and *j*+*l* specify the

neighboring grid cell where k and l can be either -1, 0 or 1. θ is calculated as the division between the difference in elevation (*h*) give in meters difference and the grid cell size (*d*), also in meters:

$$\theta_{(i+k,j+l)} = \frac{h_{(i,j)} - h_{(i+k,j+l)}}{d} \quad (8)$$

The sediment and C routing is done continuously at a daily time-step to preserve numerical stability of the model. More detailed explanation of the methods presented in this section can be found in the study of Naipal et al. (2016).

2.4 Litter dynamics

The four litter pools in the emulator are an below- and an above- ground litter pool, each split into a metabolic and structural pool with different turnover rates as implemented in ORCHIDEE (Krinner et al., 2005). The belowground litter pools consist mostly out of root residues. Both the biomass and litter pools have a loss flux due to fire as incorporated in ORCHIDEE by the Spitfire model of Thonicke et al. (2010). The litter that is not respired or burnt is transferred to the SOC pools based on the Century model (Parton et al., 1987) and the vertical discretization scheme SOC scheme presented by Naipal et al., (2018).

The vertical discretization scheme was introduced in the emulator to account for a declining C input and SOC respiration with depth, and consists of 20 layers with each 10 cm thickness. The litter to soil fluxes from above-ground litter pools are all attributed to the top 10 cm of the soil profile. The litter to soil fluxes from belowground litter pools are distributed exponentially over the whole soil profile according to:

$$I_{be}(z) = I_{0be} * e^{-r*z} \quad (9)$$

Where I_{0be} is the below-ground litter input to the surface soil layer and *r* is the PFT-specific vertical root-density attenuation coefficient as used in ORCHIDEE. The sum of all layer-dependent litter to soil fractions is equal to the total litter to soil flux as calculated by ORCHIDEE. The vertical SOC profile is modified by erosion and the resulting deposition fluxes, which is discussed in detail in the following sections.

2.5 Crop harvest and yield

We adjusted the representation of crop harvest from ORCHIDEE by assuming a variable harvest index for C3 plants that increases during the historical period as shown in the study of Hay (1995) for Wheat and Barley, which are also the main C3 crops in the Rhine catchment. The harvest index is defined by the ratio of harvested grain biomass to above-ground dry matter production (Krinner et al., 2005). In this study the harvest index increases linearly between 0.26 and 0.46 (Naipal et

al. 2018) consistent with the average values of Hay (1995). We also found that in certain cases the cropland NPP was too high during the entire period of 1850-2005, especially in the early part of the 20th Century. This is because the cropland photosynthetic rates were adjusted in ORCHIDEE to give a cropland NPP representative of present day values that are higher than for the low input agriculture of the early 20th Century. To derive a more realistic NPP for crop and barley in the Rhine catchment we used the long-term crop yield data obtained from a dataset on 120000 yield observations over the 20th century in Northeast French Départements (NUTS3 administrative division) (Schauberger et al., 2018). According to the yield data assembled by Schauberger et al. (2018), yields in Northeast France for these crops increased fourfold during the last century. Note that crop residues like straw constituted a larger fraction of the total biomass in 1850 than in 2005, but those residues were likely collected and used for animal feed, housing fuel. We did not account for this harvest of residue in the simulation of SOC.

2.6 SOC dynamics without erosion

The change in the carbon content of the PFT-specific SOC pools in the emulator without soil erosion as described by Naipal et al. (2018) (Fig 1):

$$\frac{dSOC_a(t)}{dt} = lit_a(t) + k_{pa} * SOC_p(t) + k_{sa} * SOC_s(t) - (k_{ap} + k_{as} + k0_a) * SOC_a(t) \quad (10)$$

$$\frac{dSOC_s(t)}{dt} = lit_s(t) + k_{as} * SOC_a(t) - (k_{sa} + k_{sp} + k0_s) * SOC_a(t) \quad (11)$$

$$\frac{dSOC_p(t)}{dt} = k_{ap} * SOC_a(t) + k_{sp} * SOC_s(t) - (k_{pa} + k0_p) * SOC_p(t) \quad (12)$$

Where, SOC_a, SOC_s, and SOC_p (g C m^{-2}) are the active, slow and passive SOC, respectively. The distinction of these SOC pools, defined by their residence times, are based on the study of Parton *et al.* (1987). The active SOC pool has the lowest residence time (1 - 5 years) and the passive the highest (200-1500 years). lit_a and lit_s (g C m^{-2} day^{-1}) are the daily litter input rates to the active and slow SOC pools, respectively; $k0_a$, $k0_s$ and $k0_p$ (day^{-1}) are the respiration rates of the active, slow and passive pools, respectively; k_{as}, k_{ap} , k_{pa}, k_{sa}, k_{sp} are the coefficients determining the flux from the active to the slow pool, from the active to the passive pool, from the passive to the active pool, from the slow to the active pool and from the slow to the passive pool, respectively.

The vertical C discretization scheme in the emulator assumes that the SOC respiration rates decrease exponentially with depth:

$$k_i(z) = k_{0i}(z) * e^{-re*z} \quad (13)$$

Where k_i is the respiration rate at a soil depth *z* and *re* (m^{-1}) is a coefficient representing the impact of external factors, such as oxygen availability that decreases with depth. k_0 is the respiration rate of the surface soil layer for a certain SOC pool *i*. The variable *re* is determined in such a way that the total soil respiration of a certain pool over the entire soil profile without erosion is similar to the output of the full ORCHIDEE model. Detailed description of how this is done can be found in the study of Naipal et al. (2018).

2.7 C erosion on hillslopes

In the model we assume that soil erosion takes place on hillslopes, and not in the floodplains due to the usually low topographical slope of floodplains. The factor *(1-f)* determines the fraction of the eroded soil that is deposited in the colluvial reservoirs (Fig 1). Soil erosion always removes a fraction of the SOC stock in the upper soil layer depending on the erosion rate and bulk density of the soil. The next soil layer contains less C and therefore at the following time-step less C will be eroded under the same erosion rate. To account for this effect, the SOC profile evolution is dynamically tracked in the model and updated at a daily time step, conform with the method of Wang et al. (2015). First, a fraction of the C from each soil pool in proportion to the erosion height is removed from the surface layer. Then, at the same erosion rate, SOC from the subsoil layer becomes the surface layer, maintaining the soil layer thickness in the vertical discretization scheme. Similarly, the SOC from the subsoil later also moves upward one layer. The removal of C by erosion also triggers a compensatory C sink due to the reduction in SOC respiration on eroding land. This compensatory C sink and reduced C erosion over time will ultimately lead to an equilibrium state. The change in C content due to erosion of the PFT-specific pools for hillslopes can be represented by the following equations:

$$\frac{dSOC_{HSi}(z,t)}{dt} = k_E * SOC_{HSi}(z+1,t) - k_E * SOC_{HSi}(z,t) \quad (14)$$

Where $dSOC_{HSi}(z,t)$ is the change in hillslope SOC of a component pool *i* at a depth *z* and at time step *t*. The daily erosion fraction k_E (dimensionless) is calculated as following:

$$k_E = \frac{f*\left(\frac{E}{365}\right)}{BD*dz} * EF \quad (15)$$

Where, *E* is the erosion rate (t ha^2 $year^{-1}$), *f* is the floodplain deposition factor, *BD* is the average bulk density of the soil profile (g cm^{-3}), ~~and~~ *dz* is the soil thickness (=0.1 m), and EF is the C enrichment factor that is set to 1 by default. EF>1 represents a higher C concentration in eroded soil compared to the original soil, due to the selectivity of erosion.

This part of the model has been already applied at the global scale as the C removal model presented by Naipal et al. (2018) and is here extended with the deposition term detailed above.

2.8 C deposition and transport in floodplains

The SOC profile dynamics of floodplains are controlled by: (1) C input from the hillslopes, (2) C import by lateral transport from the floodplain fractions of upstream neighboring grid cells, and (3) C export to the floodplain fractions of downstream neighboring grid cells (Fig 1). First, the net eroded flux from the surface layer of the hillslope fraction of the grid cell (k_E *SOC_{HS} (z=0)) is incorporated in the surface layer of the floodplain. At the same deposition rate, the SOC of the surface layer of the floodplain is incorporated in the subsoil layer. Similarly, a fraction of the SOC of the subsoil layer is moved downward one layer. We will refer to this process as the 'downward' moving of C in the soil layer profile. It should be noted that C selectivity during transport and deposition is not taken into account here, meaning that the C pools of the deposited material are the same as the eroded material from the topsoil of eroding areas. At the same time a fraction of the C of the surface layer proportional to the sediment residence time (τ) is exported out of the catchment following the sediment routing scheme, resulting in the 'upward' moving of the C from the subsoil layers.This process represents the river bank erosion and resulting POC export by rivers. It should be noted that rivers and streams are not explicitly represented in the model. As we do not have information on the sub-grid spatial distribution of land cover fractions we first sum the exported C flux over all PFTs before assigning the flux proportionally to the land cover fractions of the receiving downstream-lying grid cells. The C that is imported from the neighboring grid cells follows the same procedure as the deposition of eroded material, and results in a 'downward' moving of the C in the soil profile. The change in C content due to deposition and river export/import of the PFT-specific pools for floodplains can be represented by the following equations:

$$\frac{dSOC_{FLi}(z,t)}{dt} = \left(\left(k_D + k_{i_{out}}\right) * SOC_{FLi}(z-1,t)\right) + \left(\frac{1}{(\tau*365)} * SOC_{FLi}(z+1,t)\right) - \left(\left(k_D + \frac{1}{(\tau*365)} + k_{i_{out}}\right) * SOC_{FLi}(z,t)\right), \text{ for } z>0 \quad (16)$$

$$\frac{dSOC_{FLi}(0,t)}{dt} = \sum_{n=1}^{n=9}\left(k_{i_{out}}(n) * SOC_{FLi}(0,t)(n)\right) + \left(k_E * SOC_{HSi}(0,t)\right) + \left(\frac{1}{(\tau*365)} * SOC_{FLi}(1,t)\right) - \left(\left(k_D + \frac{1}{(\tau*365)} + k_{i_{out}}\right) * SOC_{FLi}(0,t)\right), \text{ for } z=0 \quad (17)$$

Where n is the neighboring grid cell that flows into the current grid cell, $dSOC_{FLi}(z,t)$ is the change in floodplain SOC of a component pool i at a depth z and at time step t, and SOC_{HS} is the hillslope SOC stock. k_D is the deposition rate and equal to:

$$k_D = \frac{k_E * AREA_{HS}}{AREA_{FL}} \quad (18)$$

Where $AREA_{HS}$ is the hillslope area and $AREA_{FL}$ is the floodplain area (m^2). $k_{i_{out}}$ is the import rate per C pool i from neighboring grid cells (dimensionless) and can be calculated as:

$$k_{i_{out}} = \frac{\sum_{n=1}^{n=9}(W * \frac{1}{\tau * 365} * AREA_{FL})\,(n)}{AREA_{FL}} \quad (19)$$

Where, W is the weight index of equation 7.

The first term of equation 16 represents the 'downward' moving of the incoming C related to the C deposition flux from the hillslope fraction of the gridcell and the lateral C import flux from the floodplain fractions of upstream neighboring grid cells. The second term represents the 'upward' moving of SOC related to the lateral C transfer to downstream neighboring grid cells. The third term of equation 16 represents the total C loss flux from the current soil layer *z*, which is a result of either the 'upward' or 'downward' moving of the C in the soil profile. The first term of equation 17 represents the incoming lateral C flux from the floodplains of the upstream neighboring grid cells. The second term represent the C deposition flux coming from the hillslope fraction of the grid cell. The third term represents the 'upward' moving of the SOC from the subsoil layer to the topsoil layer as a result of sediment/C routing. The last term of equation 17 represents the total loss of C from the topsoil layer, of which part is distributed across the neighboring grid cells downstream ($\frac{1}{(\tau * 365)}$), and another part if moved 'downwards' in the soil profile as a result of C deposition (k_D) and the incoming later C from upstream grid cells ($k_{i_{out}}$).

2.9 The land use change bookkeeping model

The land use change bookkeeping scheme includes the yearly changes in forest, grassland and cropland areas in each grid cell as reconstructed by Peng et al. (2017) (Table 1). Peng et al. (2017) derived historical changes in PFT fractions based on LUHv2 land use dataset (Hurtt et al., 2011), historical forest area data from Houghton, and present day forest area from ESA CCI satellite land cover (European Space Agency, ESA, 2014). By using different transition rules and independent forest data to constrain the changes in crop and urban PFTs he derived the most suitable historical PFT maps.

When land use change takes place, the litter and SOC pools of all shrinking PFTs are summed and allocated proportionally to the expanding PFTs, maintaining the mass-balance. In this way the litter pools and SOC stocks get impacted by different input and respiration rates for each soil layer. When forest is reduced, three wood products with decay rates of 1, 10 and 100 years are formed and harvested. The biomass pools of other shrinking land cover types are transformed to litter and allocated to the expanding PFTs. For more details on the land use scheme see the study of Naipal et al. (2018).

2.10 Study-Area

The model is tested for the Rhine catchment (Fig 2), which has a total basin area of 185,000 km^2 covering five different countries in Central Europe. Its large size is beneficial for the application of a coarse-resolution model such as CE-DYNAM to study large-scale regional dynamics in the C cycle due to soil erosion. The Rhine catchment has a very interesting topography, with steep slopes larger than 20% upstream in the Alps, and large, wide and flat floodplains at the foot of the Alps, the upper Rhine and the lower Rhine. The floodplains store large amounts of sediment and C that originally was eroded from the steep hillslopes upstream. This makes it possible to study the long-term effect of erosion on hillslope and floodplain dynamics. Furthermore, the Rhine catchment has been experiencing different stages of land use change over the Holocene, with land degradation dating back to more than 5500 years ago (Dotterweich, 2013). In contrast, during the last two decades there has been a general afforestation and soil erosion has been decreasing. These land use changes and changes in erosion make an interesting and important case to study the effect of anthropogenic activities on the C cycle in Europe.

In addition, the Rhine catchment has been the focus of many erosion studies providing observations on erosion and sediment dynamics that can be used for model validation (Asselman, 1999; Asselman et al., 2003; Erkens, 2009; Hoffmann et al., 2007, 2008, 2013a, 2013b; Naipal et al., 2016). The global sediment budget model that forms the basis for the sediment dynamics of CE-DYNAM has been validated and calibrated for the Rhine catchment with observations on sediment storage from Hoffmann et al. (2013b) and the derived scaling relationships between sediment storage and basin area (Naipal et al., 2016). Hoffmann et al. (2008, 2013) did an inventory of 41 hillslope and 36 floodplain sediment and SOC deposits related to soil erosion over the last 7500 years. The floodplain sediment observations consist mostly out of organic material (gyttja, peat) and fine sediments (fine sand, loam, silt) in overbank deposits (Hoffmann et al., 2008). These fine sediments are a result of long-term soil erosion on the hillslopes. Hoffmann et al. (2013) found that the sediment and SOC deposits were quantitatively related to the basin size according to certain scaling functions, where floodplain deposits increased in a non-linear way with basin size while the hillslope deposits showed a linear increase with basin size. ~~These scaling relationships are also applicable for SOC storage and basin area. Hoffmann et al. (2013) found that for floodplains the sediment and C storage increase in a non-linear way with basin area, while hillslopes show linear increase.~~ We will use these relationships to validate the spatial variability in SOC storage of floodplains and hillslopes simulated by CE-DYNAM. The scaling relationships have the form of a simple power law:

$$M = a * \left(\frac{A}{A_{ref}}\right)^b \quad (20)$$

Where M is the sediment storage or the SOC storage, a is the storage (Mt) related to an arbitrary chosen area A_{ref}, while b is the scaling exponent.

2.11 Input data and model simulations

To create the C emulator that forms the underlying C cycle part of CE-DYNAM, we first ran the full ORCHIDEE model for the period 1850-2005 at a coarse resolution of 2.5°degrees latitude and 3.75° degrees longitude, and output all C pools and fluxes. The pools and fluxes were then archived together and used to derive the turnover rates to build the emulator. The SOC scheme of the emulator that has been modified to account for soil erosion processes has been made to run at a spatial resolution of 5 arcmin, similar to the original global sediment budget model. Then, we performed three main simulations with CE-DYNAM for the Rhine catchment. Simulation S0: The baseline simulation or no-erosion simulation, where SOC dynamics are similar to the full ORCHIDEE model. Simulation S1: The erosion -only simulation, where the hillslopes erode and all eroded C is respired to the atmosphere without reaching the colluvial and alluvial deposition sites. Simulation S2: The simulation with full sediment dynamics where hillslopes and floodplains are connected and can bury or loose C. We ran the emulator for 32000 years at a daily time step with the initial climate and land cover of the period 1850-1860. To speed up the spin-up simulations we calculated the temporary equilibrium state of the floodplain SOC pools every 10 years analytically. At the end of the spin-up period the floodplain SOC pools were close to equilibrium, with a yearly change of less than 0.001% of the total floodplain SOC stock. Afterwards, we performed the transient simulations for the period 1851-2005 at a daily time step with changing climate and land cover conditions, using the equilibrium SOC stocks as baseline. ~~. However, after 2000 years the model the passive SOC pool was still not in complete equilibrium with a change between 0.8 and 1 g C m^{-2} $year^{-1}$. Therefore, we subtracted the additional increase in SOC stocks resulting from the disequilibrium state from the SOC stocks of the transient simulations before analyzing the transient results.~~ To ensure a faster performance of CE-DYNAM we delineated the Rhine catchment in seven~~7~~ large sub-basins based on the flow direction and ran the model in parallel for each of the sub-basins at a~~the~~ daily timestep. After each year the sub-catchments exchanged the lateral C fluxes with ~~between~~ each other.

We also performed seven additional sensitivity simulations and four additional uncertainty simulations. Simulation S1_EF and S2_EF are performed to test the model assumption of a C enrichment during erosion. Here, we changed the enrichment factor EF to two, based on the study of Lugato et al. (2018). Simulations S2_Tmin and S2_Tmax are performed to test the rate of C transport between floodplains. Here we modified the average sediment residence time for the Rhine catchment to a minimum of 60 years (50 % lower than the current value), and to a maximum of 128 years (50% higher than the current value), respectively. However, we kept the maximum sediment residence time at 1500 years. Simulations S0_RM, S1_RM and S2_RM are performed to test the model assumption on crop residue management, where we assumed that all above-ground crop litter is harvested.

For the uncertainty analysis we performed simulations S1_min and S2_min based on a minimum soil erosion scenario, and S1_max and S2_max based on a maximum soil erosion scenario. These soil erosion scenarios are based on the uncertainty ranges in the rainfall erosivity and land cover factors of the erosion model. All the model simulations are summarized in table 2.

2.12 Validation methods and data

We performed a detailed model validation of the sediment and the C part of the model based on the following steps: (1) validation of soil erosion rates using observational and high-resolution model estimates for Germany and Europe, (2) validation of C erosion rates using high-resolution model estimates for Europe from Lugato et al. (2018), (3) validation of the spatial variability of hillslope and floodplain C storage using observational results from Hoffmann et al. (2013), (4) validation of SOC stocks using observational data from a global soil database and a European land use survey.

The validation of the soil erosion module has been done before in the studies of Naipal et al. (2015, 2016). However, we do it again in this study due to different input datasets. For the validation of gross soil erosion rates we used the high-resolution model estimates from the study of Panagos et al. (2015), who applied the RUSLE2015 model at a 100 m resolution at European scale for the year 2010. The RUSLE2015 is derived from the original RUSLE model with some modifications to the model parameters L, C and P. The erosion module of CE-DYNAM is also based on a modified version of the RUSLE (Adj.RUSLE) which , however, lacks the L and P factors. It calculates the potential soil erosion rate under the assumption of no erosion control scenarios, in contrast to RUSLE2015, which does represent erosion control practices. Adj.RUSLE also differs from RUSLE2015 in the use of more coarsely resolved input datasets (table 1), for which the equations for the R and S factors have been modified. The extensive validation of the Adj. RUSLE model in this study and previous studies (Naipal et al., 2015, 2016, 2018), shows that despite its coarse resolution, the methodology works for large spatial scales. In contrast, RUSLE2015 uses largely similar equations as in the original RUSLE model presented in Renard et al. (1997). Thus, even though both Adj.RUSLE and RUSLE2015 are derived from the same erosion model, the differences between the models are large, and would justify our model comparison. Furthermore. we used independent high-resolution erosion estimates from the study of Cerdan et al. (2010), available at a 1 km resolution at European scale, which were based on an extensive database of measured erosion rates under natural rainfall in Europe. For the comparison we aggregated the high-resolution model results of both datasets to the resolution of CE-DYNAM. We also used the potential soil erosion map of the Federal Institute for Geosciences and Natural Resources of Germany (Bug and Stolz, 2014). This map presents the yearly average soil erosion rates at 250 m resolution on agricultural land derived from a USLE-based approach, with some modifications to the erosion factors and input data. Before validating our model results we also aggregated these high-resolution erosion rates to the coarser resolution of our model.

Validation of our net soil erosion rates is done based on the 100 m resolution net soil erosion rates derived with the WATEM-SEDEM model (Borrelli et al., 2018). WATEM-SEDEM simulates soil removal by water erosion based on the USLE approach, sediment transport and deposition based on the transport capacity. The model has been extensively employed to estimate net fluxes of sediments across hillslopes at, catchment- and regional-scale level.

For the validation of C erosion rates, we used the high-resolution model results from Lugato et al. (2018), where they coupled the RUSLE2015 erosion model to the Century biogeochemistry model. These model results were available at a

519 resolution of 1km, where each gridcell was composed of an erosion and a deposition fraction. The C erosion rates provided
520 by Lugato et al. (2018) were multiplied with the erosion fraction of a 1 km grid cell. Then, the C erosion rates were
521 aggregated to the resolution of CE-DYNAM. Lugato et al. (2018) provided an enhanced and a reduced erosion-induced C
522 sink uncertainty scenario, based on different assumptions for C enrichment, burial and C mineralization during transport. In
523 CE-DYNAM the C erosion rates from simulation S1 are multiplied with the hillslope area to get the total C erosion flux of
524 a grid cell. As the study of Lugato et al. (2018) considers only agricultural areas, we considered only the crop fraction of a
525 grid cell. It should be noted that the SOC dynamics scheme of CE-DYNAM, which is derived from ORCHIDEE LSM, is
526 based on the Century model. However, there are large differences between the Century model used by Lugato et al. (2018)
527 and the C dynamics scheme of ORCHIDEE used in this study. For example, in the Century model the crop productivity is
528 mediated by nitrogen availability, which is not the case in the ORCHIDEE version used for this study. The Century model
529 also includes some management practices such as crop rotations, which are not represented in ORCHIDEE. The Century
530 model runs at a much higher resolution and is calibrated for agricultural land, while ORCHIDEE also simulates forest,
531 grasslands and bare soil. In this way, the final SOC stocks derived with CE-DYNAM are also a result of erosion from other
532 land cover types and land use changes. This is an important feature for land use change, which is not included in the
533 Century model. Furthermore, the ORCHIDEE LSM has been used in many global intercomparisons and extensively
534 evaluated for C budgets (Mueller et al., 2019; Todd-Brown et al., 2013). Also an important advantage of ORCHIDEE is
535 that it includes the last century change in crop production calibrated against data (Guenet et al., 2018).
536
537 For the validation of the spatial variability of the SOC stocks of hillslopes and floodplains we used the scaling relationships
538 between basin area and SOC storage derived by Hoffmann et al. (2013) (Section 2.10). The study by Naipal et al. (2016)
539 found that the global sediment budget model is able to reproduce the scaling parameters for sediment storage, and after
540 analyzing the dependence of the scaling behavior on the main parameters of the model, they argue that the scaling is an
541 emergent feature of the model and mainly dependent on the underlying topography. This indicates that the scaling features
542 of floodplain and hillslope sediment and C storage should also be applicable to the more recent time period, such as in our
543 study. In our study we aim to evaluate the ability of CE-DYNAM to reproduce this scaling behavior for the SOC storage of
544 the Rhine. For this purpose we selected the grid cells that contained the points of observation of the study of Hoffmann et
545 al. (2013) and performed a regression of the basin area (defined as the upstream contributing area) and the SOC storage of
546 that gridcell for floodplains and hillslopes separately. Comparing the absolute values of the sediment and SOC storages of
547 each grid cell from Hoffmann et al. (2013) was not possible due to the difference in the time-period of the studies, where
548 Hoffmann et al. (2013) focussed on the entire Holocene, while our study focussed only on the period starting from 1850
549 AD.
550
551 For the validation of the total SOC stocks we used the Global Dataset for Earth System Modeling (GSDE) (Shangguan et
552 al., 2014) available at a spatial resolution of 1 km and the Land Use/Land Cover Area Frame Survey (LUCAS) (Palmieri et
553 al., 2011). The LUCAS topsoil SOC stocks, available at a high spatial resolution of 500 m, were calculated using the

LUCAS SOC content for Europe (de Brogniez et al., 2015) and soil bulk density derived from soil texture datasets (Ballabio et al., 2016).

3 Results

Due to large uncertainties in the model and validation data for the Alpine region we only present and discuss the model and validation results for the non-Alpine part of the Rhine catchment.

3.1 Model validation

In this section we present the model validation results using the methods and validation data described in detail in the previous section. ¶

~~We performed a detailed model validation of the sediment and the C part of the model based on the following steps: (1) Validation of soil erosion rates using high-resolution model estimates and observations from other studies, (2) validation of C erosion rates using high-resolution estimates for Europe from the study of Lugato et al. (2018), (3) validation of the spatial variability of sediment storage, (4) validation of SOC stocks using data from a global soil database and a European land use survey.~~

~~For the validation of gross soil erosion rates we used the high-resolution model estimates from the study of Panagos et al. (2015), who applied the RUSLE2015 model at a 100 m resolution at European scale for the year 2010. The RUSLE2015 is derived from the original RUSLE model with some modifications to the model parameters, especially the L, C and P factors. We also used independent high-resolution erosion estimates from the study of Cerdan et al. (2010), which were based on an extensive database of measured erosion rates under natural rainfall in Europe.~~

We find that the quantile distribution of the simulated gross soil erosion rates compares well to ~~fall in between~~ the ~~estimated~~ distributions~~s~~ of ~~these~~ other observational and high-resolution modelling studies (Cerdan et al., 2010, Panagos et al., 2015, Bug et al., 2014) ~~two studies~~ (Fig 3A, B, C~~&B~~). It should be noticed that our study, ~~and~~ the study of Cerdan et al. (2010) and Bug et al. (2014) simulated potential soil erosion rates, not accounting for erosion control practices that are captured by the P-factor. We also find that ~~compared~~ the quantile distribution of the simulated net soil erosion ~~rates~~ from hillslopes in our study compares well with the distribution from the high-resolution modelling ~~ose of the~~ study of Borrelli ~~Lugato~~ et al. (2018)~~, and show that they are similar~~ (Fig 3D~~C~~). Furthermore, we performed a spatial comparison of our simulated gross and net erosion rates to those of the studies mentioned above. For this purpose we delineated 13 sub-basins in the Rhine catchment (Fig S3). Table 3 summarizes the resulting goodness-of-fit statistics of this comparison and shows that our erosion model is generally in good agreement with the other studies at sub-basin level. ~~Lugato et al. (2018) extended the RUSLE2015 model with a hillslope sediment deposition and transport scheme based on the sediment delivery ratio concept.~~ ¶

¶

For the comparison of the spatial variability of gross soil erosion rates we used the relationship of erosion to the topographical slope and rainfall erosivity. These two parameters are argued to explain about 70% of the total potential soil erosion rates at regional scales (Doetterl et al., 2012). We show that in our study and the study of Lugato et al. (2018) erosion rates increase with increasing slope and erosivity, and that erosion can be high for very steep slopes with a low erosivity (Fig 4). However, the difference between small and large erosion rates in our study is high, indicating an underestimation of local variability in erosivity and slope. Overall, our results show that our coarse-resolution erosion model is capable of producing reliable estimates of potential soil erosion rates and their spatial variability for the Rhine catchment.¶

For the validation of gross C erosion rates, we used the results from Lugato et al. (2018), where they coupled the RUSLE2015 erosion model to the Century bio-geochemistry model. They provided an enhanced and a reduced erosion-induced C sink uncertainty scenario, based on different assumptions for C burial and C mineralization during transport. WWe find that the quantile distributions of our simulated agricultural carbon erosion and deposition rates areis similarclose to thoseat of the high-resolution modelling study of Lugato et al. (2018) (Fig 45A-D). Also the spatial variability of the C erosion rates at sub-basin level is in good comparison to the validation data (table 4). However, Wwe also find that the linear regression relationship between soil erosion and C erosion rates of our study lies at the lower end of the relationships derived from the enhanced and reduced uncertainty erosion scenarios of is similar to the relation of Lugato et al. (2018) and falls within the uncertainty range (Fig 56). This could be explained by the fact that we do not explicitly consider erosion-control and management practices on agricultural land, and the coarse resolution of our model. T The coarse resolution of our model may explain the decreased spread in variability between our simulated values is also a result of the estimateis as can be explained by t the coarse resolution of our model.

For the validation of SOC stocks we used the Global Dataset for Earth System Modeling (GSDE) (Shangguan et al., 2014) available at a spatial resolution of 1km and the Land Use/Land Cover Area Frame Survey (LUCAS) (Palmieri et al., 2011). The LUCAS topsoil SOC stocks, available at a high spatial resolution of 500 m, were calculated using the LUCAS SOC content for Europe (de Brogniez et al., 2015) and soil bulk density derived from soil texture datasets (Ballabio et al., 2016). We find that t Accounting for erosion, deposition and transport of SOC leads to a better representation of the simulated topsoil C stocks per land cover type when comparing to SOC stocks of the LUCAS database (Fig 6). The simulated top 20 cm SOC stocks of the top 20 cm of the soil profile per land cover type generally fall within the quantile range of the LUCAS SOC stocks for cropland and forest (Fig 67). The topsoil SOC stocks for grassland improve but still show a large uncertainty range. We also find that the simulation with erosion does not substantially change this result but leads to slightly lower SOC stocks due to the impact of erosion and POC export out of the catchment. Furthermore, we find that in both the erosion and no-erosion simulation the SOC stocks for grassland are higher than for forest. This is also observed in the study of Wiesmeier et al. (2012) in South-Germany where they found considerable higher SOC stocks for grassland with a median of 11.8 kg C m^{-2} compared to forest based on the analysis of 1460 soil profiles. Furthermore, the comparison of To validate the spatial variability of the simulated total SOC stocks to those of the LUCAS and GSDE databases we

delineated 13 sub-basins in the non-Alpine region. at sub-basin level shows a good model performance with respect to the We found a realistic spatial variability in topsoil SOC stocks after comparing our simulated SOC stocks from the erosion simulation with the SOC stocks of GSDE and LUCAS at sub-basin level (Table 52). To validate the spatial variability of floodplain and hillslope SOC stocks separately, we used the scaling relationships found by Hoffmann et al. (2013) (section 2.12). For this purpose we ¶

¶

For the validation of sediment storage in hillslopes and on floodplains we used the same approach as in Naipal et al. (2016), where we based our validation on measured Holocene sediment and SOC deposits from the study of Hoffmann et al. (2008, 2013). These studies contain an Hoffmann et al. (2013) did an inventory of 41 hillslope and 36 floodplain sediment and SOC deposits related to soil erosion over the last 7500 years. The floodplain sediment observations consist mostly out of organic material (gyttja, peat) and fine sediments (fine sand, loam, silt) in overbank deposits (Hoffmann et al., 2008). These fine sediments are a result of long-term soil erosion on the hillslopes. Hoffmann et al. (2013) found that They found that the sediment and SOC deposits were related to the basin size according to certain scaling functions, where floodplain deposits increased in a non-linear way with basin size while the hillslope deposits showed a linear increase with basin size. We selected the grid cells that contained the points of observation of the study of Hoffmann et al. (2013). with We and found We find ith CE-DYNAM we derived a a significantly larger exponent forof the scaling relationship between the simulated floodplain SOC storage and basin area compared to the simulated hillslope SOC storage, when using the grid cells that contain the points of observation corresponding to the study of Hoffmann et al. (2013). This result is in line with what Hoffmann et al. (2013) found and shows that CE-DYNAM can realistically reproduce the spatial variability in SOC stocks between hillslopes and floodplains (table 6). which corresponds to the findings of Hoffmann et al. (2013). However, this is not the case when deriving the scaling relationships at sub-basins level instead of using individual grid cells we do not find a significant difference in scaling between floodplains and hillslopes (tTable 63).

3.2 Model application

We find an average annual soil erosion rate of 1.444.66±0.82 t ha^{-1} year^{-1} over the period 1850-2005, which is about half of the 1.7 times larger than the average erosion rate simulated for the last millennium (Naipal et al., 2016) and falls into the range of 3.8 times larger than the average erosion rate of the Holocene (Hoffmann et al., 2013). This soil erosion flux mobilized around 661±2859 Tg of C over the period 1850-2005, of which on average about 5737% is deposited in colluvial reservoirs, 4363% is deposited in alluvial reservoirs, while and 0.2% is exported out of the catchment.

The lower average annual soil erosion rate over the study period compared to the last millennium is a result of the Over the period 1850-2005 there is a general afforestation in the non-Alpine part of the Rhine catchment that started around 19120 AD (Fig 78B). Land cover data shows that forest increases by 24% over the period 1910-2005, mostly as a result of grassland to forest conversion. Cropland decreases by 6% over the period 1920 and 1970, and is relatively stable

afterwards. This afforestation takes place in the non-Alpine part of the Rhine and leads to a long-term decreasing trend in gross soil and SOC erosion rates on hillslopes in the non-Alpine region (Fig 78CD). In the Alpine part of the Rhine there was a conversion of cropland and forest to grassland. Cropland decreases by 1875% over the period 1920 and 1960, while forest indecreases by 2416% over the period 1910-20051950. Over the period 1940-1960 erosion rates increase suddenly due to increased precipitation . The conversion of forest to grassland has a stronger impact on the soil erosion rates than the conversion of cropland to forest, resulting in an increase of soil erosion rates over the period 1910-1950 (Fig 8C). This increase is amplified by increased yearly precipitation in this region. Because the soil erosion rates in the Alps are generally much larger than the soil erosion rates in the non-Alpine region due to the steep landscape, the Alpine region dominates the trend in gross soil erosion and C erosion of the entire in the period 1910-1950 (Fig 8C). As a result, the summed gross soil and C erosion rates over the whole Rhine catchment do not show a specific trend (Fig 8C). T The temporal variability in the soil and C erosion rates is a result of direct changes in precipitation, such as the temporary increase in erosion rates over the period 1940-1960 (Fig 7A). (Fig 8A), however, land use change dominates the overall long-term trend. Although precipitation is temporarily very variable, spatially it does not vary significantly over the Rhine. ¶

¶

Furthermore, we find that the temporal variability in C erosion rates follow the soil erosion rates closely, indicating that soil erosion dominates the variations in C erosion over this time-period, while increased SOC stocks due to CO_2 fertilization and afforestation play a secondary role as a slowly, varying trend. It should be noted that the correlation between soil and C erosion might be affected by processes not properly captured by the model such as the selectivity of erosion, which also include the enrichment of C in eroded material.

TWe find that the cumulative C erosion removal flux of 66159±28 Tg of C leads to a cumulative net C sink for the whole Rhine region of 216±2390 Tg C (Fig 78DE). This is about 2.1 – 2.7 % of the cumulative NPP and of the same magnitude as the cumulative land C sink of the Rhine without erosion. , which is about 1% of the cumulative NPP and about one fourth of the cumulative land C sink of the Rhine without erosion. For the non-Alpine part of the Rhine erosion leads to a net C sink of 55 Tg C, which equals to one fifth of the total land C sink without erosion. It should be noted that these are potential fluxes, assuming that the photosynthetic replacement of C is not affected by the degradation of soil due to the removal of nutrients, declining water-holding capacity and other negative changes to the soil structure and texture (processes not covered by our model). The breaking point in the graphs of figure 78DE and F around 1910 AD is a result of the climate data used as input.

To better understand the erosion-induced net C flux (Fig 78DE, F), we analyzed the erosion-induced C exchange with the atmosphere by creating C budgets for the entire Rhine catchment for the period 1850-1860 and for the period 1950-2005 (Fig 89A&B). These C budgets also shed light on changes in the linkage between lateral and vertical C fluxes over time. As we do not explicitly track the movement of eroded C through all reservoirs (for example between eroding hillslopes and colluvial reservoirs), we make use of the changes in SOC stocks and NEP of the three main simulations (S0, S1, S2) to derive the erosion-induced vertical C fluxes. By subtracting the Net Ecosystem Productivity of hillslopes (NEP_{HS}), which is

the difference between NPP and heterotrophic respiration, of the no-erosion simulation (S0) from the erosion-only simulation (S1), we derive the additional photosynthetic replacement of SOC on eroding sites (Eq. 21):

$$E_{rep} = NEP_{HS}(S1) - NEP_{HS}(S0) \quad (21)$$

Where, E_{rep} is the potential dynamic Photosynthetic replacement of C on eroding sites (assuming no feedback of erosion on NPP). Part of the eroded C that is transported to and deposited in colluvial reservoirs can be respired or buried (Eq. 22). The difference between NEP of simulation S2 and S1 is the NEP caused by the deposition of eroded C in colluvial areas and equal to the difference between the burial and respiration of C in colluvial sites. As we do not explicitly track the respiration of deposited material in the model, we can only derive the net respiration or net burial of the colluvial deposits (Rc_{net}) with the following equation:

$$Rc_{net} = NEP_{HS}(S2) - NEP_{HS}(S1) \quad (22)$$

The same concept can be applied for the net respiration of floodplains:

$$Ra_{net} = NEP_{FL}(S2) - NEP_{FL}(S0) \quad (23)$$

Where, NEP_{FL} is the floodplain Net Ecosystem Productivity, and Ra_{net} is the net respiration or net burial of alluvial deposits. Positive values for Ra_{net} or Rc_{net} indicate a net burial (respiration S2 < respiration S0/S1) of the deposited material.

We find that the dynamic replacement of C on eroding sites increased by 17-33%~~39%~~ at the end of the period despite decreasing soil erosion rates (Fig 8~~9~~A&B). This increase in the photosynthetic replacement of C is due to the globally increasing CO_2 concentrations that lead to ~~known as~~ the CO_2 fertilization effect, amplified by the afforestation trend in the Rhine over this period. Without this fertilization effect, soil erosion and deposition would be likely a weaker C sink or even a C source over the period 1850-2005 (Fig S4 A&B). This CO_2 fertilization effect promotes a 100% replacement of the eroded C on hillslopes and even leads to a C sink on hillslopes at the end of the study period (Fig 8B). Furthermore, we find that the yearly average gross C erosion flux from eroding sites decreases ~~slightly~~ by 10-34~~2~~%, while the yearly deposition fluxes in colluvial and alluvial sites decreases by 20~~3.5~~ % and 19-47~~0.6~~%, respectively. The decrease in the deposition flux to floodplains is compensated by a better sediment connectivity between hillslopes and floodplains due to afforestation. Forests have less man-made structures that can prevent the erosion fluxes from reaching the floodplains, which is represented by a higher floodplain deposition '*f*' factor in the model. The decrease in the erosion flux also leads to a decreased POC export of the catchment at the end of the study period.

We also find that both the colluvial and alluvial reservoirs show a net respiration flux throughout the time period (Fig 89A&B). This is consistent with previous studies who found that deposition ~~colluvial~~ sites can be areas of increased CO_2 emissions (Billings et al., 2019; Van Oost et al., 2012). However, there is a slight difference in the respiration of deposited C between the start and end of the transient period. The respiration of deposited SOC in colluvial sites increases with time while the respiration of deposited SOC in alluvial sites shows rather a decreasing trend. These changes in SOC respiration of deposited material depend on (1) the amount of deposited material, (2) increasing temperatures over 1850-2005 for the entire catchment, and (3) the constant removal of C-rich topsoil and its deposition in alluvial and colluvial reservoirs, which makes the deposited sediments generally richer in C than soils on erosion-neutral sites, providing more substrate for respiration. ~~This decreasing trend in SOC respiration of alluvial material depends on the erosion strength and the sediment connectivity between hillslopes and floodplains.~~ ~~is triggered by the net respiration/burial flux of deposited C in floodplains. While at the start of the period, deposition in alluvial reservoirs leads to a substantial net burial flux (~0.8 times the floodplain deposition), at the end of the period respiration of deposited SOC in floodplains is larger than this burial flux (Fig 9B). These trends in respiration of deposited material are furthermore controlled by two main processes, (1) a general increase in respiration~~ This is a result of an increased respiration of deposited material over the entire catchment, most likely due to increasing temperatures over 1850-2005 ~~for the entire catchment, and (2)~~ . ~~T~~the constant removal of C-rich topsoil and its deposition in alluvial and colluvial reservoirs, which makes the deposited sediments generally richer in C than soils on erosion-neutral sites, providing more substrate for respiration. The largest increase in total respiration of alluvial and colluvial deposits takes place in hilly regions ~~the Alps~~ due to the initial increase in erosion rates resulting in large deposits of C.¶

¶

~~We also observe declining erosion rates over the non-Alpine region leading to decreasing or less strong increasing dynamic replacement of C. Both processes, T~~t Overall, we find that the increased respiration of deposited material slightly offsets the increased ~~decrease in burial~~ dynamic C replacement, however, the dynamic C replacement on eroding sites still dominates the erosion-induced C sink. ~~, leading to a constant~~ contribute to a reduced increase in the erosion-induced net C sink over time (Fig 8~~D~~E, F).¶

4 Discussion

In this chapter we discuss some of the most important model limitations, uncertainties and assumption.

4.1 Initial conditions and past global changes

Initial climate and land cover/use conditions needed to perform the equilibrium simulation together with the length of the transient period are essential parameters that determine the resulting spatial distribution of soil and C. Landscapes are in a constant transient state due to global changes, such as climate change, land use change, accelerated soil erosion. However,

we assumed an equilibrium state so that we can quantify the changes during the transient period. The more one goes back in time to select the initial conditions and the longer the transient period that covers the essential historical environmental changes, the more accurate are the present-day distribution of SOC stocks, sediment storages, and related fluxes. This is especially true when analyzing the redistribution of soil and C as a result of erosion, deposition and transport, as these soil processes can be very slow. For example, the study of Naipal et al. (2016) shows that by simulating the soil erosion processes for the last millennium a spatial distribution of sediment storages that is similar to observations can be found. In this study we modeled steady state initial conditions of the period 1850-1860 due to constraints in data availability on precipitation and temperature, and because the aim of this study is to present the potential and limitations of the new model CE-DYNAM rather than provide precise values for soil and C stocks and fluxes. By focusing only on the period 1850-2005 we miss the effects of significant land use changes in the past that coincided with times of strong precipitation such as in the 14th and 18th century. These major anthropogenic changes in the last Holocene substantially affected the present-day spatial distribution and size of SOC stocks.

As a result, our model shows that floodplains store less SOC than hillslopes. However~~As a result~~, we do find that floodplains have an overall higher C concentration (12 kg m^{-2}) compared to ~~store overall more less SOC than~~ hillslopes (9 kg m^{-2}) at the end of the transient period (Fig 9~~10~~A), which is in line with ~~different from~~ the findings of Hoffmann et al. (2013) and what can be derived from global soil databases. This is a result of higher SOC concentrations in deeper soil layers of floodplains compared to hillslopes (Fig 9 A & B). ~~also what~~ Hoffmann et al. (2013) ~~found~~.Although, the difference in C concentrations between floodplains and hillslopes is not as significant as is shown in the study of Hoffman et al. (2013). This is due to the absence of ~~because our model does not capture the~~ ~~showed that the large amount of C stored in the deeper layers of the floodplains can be several thousands of years old. In addition, the high C stocks in floodplains also result from~~ a higher local plant productivity resulting from ~~due to~~ favorable soil nutrient and hydrological conditions in our modelled floodplains. ~~In our study we do not capture this effect and we do not look at a timescale long enough to capture this distinction between SOC storage in floodplains and in hillslopes. However, we did not find that the vertical distribution of C in floodplain sediment is more homogenous or shows a less strong decrease in C with depth (Fig 10B). This is in line with the findings of previous studies (Hoffmann et al., 2013; Billings et al., 2019).~~

4.2 Model advantages and limitations

Although we parameterized and applied CE-DYNAM for the Rhine catchment, it is intended to be made applicable to other large catchments globally. CE-DYNAM combines soil erosion processes, for which small scale differences in topography are of utter importance, with a state-of-the-art representation of large-scale SOC dynamics driven by land use and environmental factors (climate, atmospheric CO_2) as simulated by the ORCHIDEE LSM. The flexible structure of CE-DYNAM makes the model adaptable to the SOC dynamics of other LSMs. In this way it is possible to study the main processes behind the linkages between soil erosion and the global C cycle.

~~Although~~ CE-DYNAM explicitly account~~s~~ for hillslope and floodplains re-deposition, which is to our knowledge unique for a large-scale C erosion model and highly novel. However, it still lacks ~~neglects~~ important processes affecting the C dynamics in floodplains. The model does not account for a slower respiration rate due to low-oxygen conditions, physical and chemical stabilization (Berhe et al., 2008; Martínez-mena et al., 2019) or a higher NPP for nutrient-rich floodplains (Van Oost et al., 2012; Hoffmann et al., 2013). The oxidation and preservation of C in deposition environments, especially in alluvial reservoirs remain highly uncertain (Billings et al., 2019).

Due to its simplistic nature and coarse-resolution, CE-DYNAM does not resolve rivers and streams explicitly but assumes that they are included in the floodplain parts of the grid cells. CE-DYNAM has been developed and calibrated to simulate long-term changes in sediment and carbon storage on land and not the short-term variations in sediment and POC fluxes carried by rivers. This limits the application of CE-DYNAM in its current form to accurately quantify sediment and POC fluxes of rivers and streams. CE-DYNAM produces a sediment export flux at the end of the year 2005 of about $1.6x10^7$ tonnes per year, which is a magnitude higher than the measured suspended sediment flux of about $3.15x10^6$ tonnes per year (Asselman et al., 2003). The higher sediment flux is the result of absent riverine processes in CE-DYNAM such as river embankment, sediment burial behind dams, and the fact that we assume an equilibrium state for the Rhine catchment based on the period 1850-1860 where agricultural soil erosion rates were already high. The simulated total cumulative sediment export of 2.5 Gt for the Rhine over the period 1850-2005 is about 36 % of the cumulative gross soil erosion flux of 6.8 Gt. This sediment flux leads to a cumulative POC export of about 0.14 Tg of C for the Rhine over the period 1850-2005. This is 0.2 % of the cumulative C erosion flux. The yearly POC flux at the end of the year 2005 is 0.02 t C km^2 $year^{-1}$ (normalized over the total basin area), which is an order of magnitude lower compared to other studies who found a total POC export for the Rhine of about 0.9 tC km^2 $year^{-1}$ (Beusen et al., 2005; Sorribas et al., 2017). This underestimation in POC in CE-DYNAM is most likely a result of the high sediment residence time of floodplains downstream of the Rhine and the absence of increased plant productivity of floodplains, leading to the decomposition of a large fraction of the deposited C. Increased plant productivity of floodplains is shown to contribute significantly to the higher SOC stocks of floodplains compared to hillslopes, and to the export of DOC and POC to rivers (Van Oost et al., 2012; Hoffmann et al., 2013). In addition, the model lacks processes that account for the transformations between POC, DOC and CO_2 and their fate in rivers and streams. The model also assumes a ‘natural’ state of the catchment where there is no river embankment and the floodplains are more or less dynamic. This may affect the behaviour of the POC export and residence time of C in floodplains.

Furthermore, the model does not take into account the full effects of the selectivity of erosion, often expressed as the enrichment ratio, where the C content of eroding soil or the deposited sediment can be different from that of ~~higher than that of~~ the original soil. The enrichment ratio can be very variable across landscapes, while the importance of erosion

selectivity for C is still under debate (Nadeu et al., 2015; Wang et al., 2010). However, we did a simple sensitivity test to study the effect of C enrichment by erosion (section 4.3).

CE-DYNAM does not account for different ratios between the SOC pools (active, slow, passive) with depth due to the limitation in information to constrain these fractions for floodplains and hillslopes. However, this can be potentially important for respiration of C in depositional sites and during transport. Studies show that the labile C is decomposed first during sediment transport and directly after deposition, leaving behind the more recalcitrant C in deposition sites (Berhe et al., 2007; Billings et al., 2019). Due to the simplistic nature of our coarse-resolution model and the lack of data on oxidation of eroded C during transport we did not include C respiration during transport in the model.

The current SOC scheme of CE-DYNAM does also not account for different residence times of SOC as a function of landscape position along a hillslope. The SOC decomposition rates can vary significantly along a hillslope due to changes in soil moisture, temperature, aggregation, and the transport of minerals and nutrients (Doetterl et al., 2016). Currently, these processes are not resolved in coarse resolution LSMs, contributing to the uncertainty in the large-scale linkage between soil erosion and SOC dynamics.

~~We also do not take into account the transformation of POC to DOC and their fate in rivers and streams. The model also lacks dams in and fixed river banks of the Rhine river. In this way, CE-DYNAM provides only a potential state of soil and SOC redistribution as would be under more natural conditions.~~ Furthermore, there is no feedback between soil erosion and plant productivity in the model. To account for such process soil erosion processes would need to be explicitly included in a land surface model such as ORCHIDEE, which would increase the computational complexity of the simulations substantially. The lack of this feedback results in an unlimited dynamic replacement of C on eroding sites.

Currently, the erosion module of CE-DYNAM does not include the L (slope-length) and P (support-practice) factors. This might induce some bias in the results, especially for agricultural land. In our next study we aim to make CE-DYNAM better applicable for agricultural land, where these factors play an important role. For this purpose we will focus on the development of new methods that can quantify the L and P factors reliably at the global scale, and will need to re-calibrate the erosion module of CE-DYNAM, the Adj.RUSLE. Our decision of leaving out the L and P factors from the erosion equation in our study is based on the global study of Doetterl et al. (2012), which showed that the S, R, C and K factors explain approximately 78% of the total erosion rates on cropland in the USA. This indicates that on cropland the L and P factors, which are related to agriculture and land management, contribute only for 22 % to the overall erosion rates. This percentage is comparable to the uncertainty range in the estimation of the S, R, C and K factors at the regional scale from coarse resolution data. Renard and Ferreira (1993) also mention that the soil loss estimates are less sensitive to slope length than to most other factors. Furthermore, various studies argue that the estimation of the L factor for large areas is complicated and thus can induce significant uncertainty in soil erosion rates calculated based on coarse resolution data (Foster et al., 2002; Kinnell, 2007). Especially, for natural landscapes, such as forest, the estimation of the L factor is not straightforward as these natural landscapes usually include steep slopes (Elliot, 2004). In order to stay consistent with the

872 estimation of potential soil erosion for all land cover types, we removed the L factor from the equation. The Adj.RUSLE
873 has been already successfully validated at the regional scale, without the L and P factors where the spatial variability of soil
874 erosion rates compares well to other high resolution modeling studies and observational data and the absolute values fall
875 within the uncertainty ranges of those validation data (Naipal et al., 2015; Naipal et al., 2016; Naipal et al., 2018; and this
876 study). Finally, the aim of this study was to develop and validate a carbon erosion module for applications at the global
877 scale, where the estimations of the L and P factors is even more limited. By showing that the erosion rates from the
878 Adj.RUSLE and CE-DYNAM are within the uncertainty of other data and modelling studies, we can assume that it will be
879 applicable for other large catchments in the temperate region.
880
881 Finally, CE-DYNAM considers only the rather 'slow' rill and interrill soil erosion processes, and does not take into
882 account gully erosion and landslides, which are bound to extreme precipitation events. The daily timestep of CE-DYNAM
883 and the current setup of the sediment budget module allows only for long-term yearly average changes in erosion and
884 deposition rates and cannot be applied to estimate episodic erosion and deposition events.
885
886 **4.3 Sensitivity analysis**
887
888 We analyzed the effects of the following model assumptions: (1) C enrichment during erosion, (2) the floodplain sediment
889 residence time, and (3) crop residue management.
890
891 To test the C enrichment we increased the EF (Eq. 15) from 1 to 2, assuming a strong enrichment of C during erosion
892 (section 2.11). We find that this enrichment results in a gross C erosion flux that is 1.61 times larger compared to the flux
893 without enrichment (table 7). This leads also to a larger dynamic replacement of C on eroding sites in combination with a
894 larger burial in depositional sites, which is in accordance with the study of Lugato et al. (2018). The resulting C sink from
895 the enrichment simulation is 1.25 times larger than the sink under default conditions. However, we do not find a significant
896 effect on the cumulative POC flux under C enrichment (table 7).
897
898 To test the potential effects of a different sediment residence time on the SOC dynamics, we performed a sensitivity study
899 where we changed the basin average sediment residence time to be 50% higher or 50% lower but keeping the maximum
900 sediment residence time at 1500 years (section 2.11). By changing the average sediment residence time and keeping the
901 maximum fixed, it will be the grid cells with the lowest residence times that will undergo the largest changes in residence
902 time and consequently in the floodplain SOC storage and export. The higher the residence time, the longer the deposited
903 soil C will reside in the floodplains, where it can either be respired or buried in deeper soil layers. Therefore, we find that
904 the effects of the sediment residence time on the SOC dynamics are non-linear. Under default conditions we find the
905 highest SOC storage. A 50% higher average sediment residence time leads to the lowest total SOC storage, with a decrease
906 of 30% compared to default conditions, while the erosional C sink is reduced by 20% (table 7). This could be explained by
907 a higher C decomposition flux for floodplains due to the long residence time of C in deposition areas. Especially, in

mountainous regions where the soil erosion flux is large and removes a large part of the labile C, a higher sediment residence time will lead to higher C decomposition emissions in floodplains. The turnover seems to dominate over the C burial in deeper layers and export. A 50% lower average sediment residence time also leads to a decrease (of 8%) in the total SOC storage and a decrease of 6% in the erosional C sink compared to default conditions (Table 7). Also here, the largest changes are found in mountainous regions where a low sediment residence time leads to a large export of C, which is then deposited in lower lying, more extensive floodplains. Thus, increasing or decreasing the residence time leads to a smaller total SOC storage, resulting from different spatial distributions of this SOC storage. The POC flux under the low sediment residence time scenario is substantially higher than under default conditions (Table 7).

To test the effects of crop residue management we harvest all above-ground crop residues (section 2.11). We find that total litter C stock is about 15% smaller compared to the default case by the end of the year 2005. This leads to a total change in the transient SOC stocks that is 20% smaller under no erosion (S0), and 26% smaller under erosion (S2) (table 7). Our findings confirm that soil management practices such as residue management have a substantial effect on the SOC dynamics.

5 Conclusions

We presented a novel spatially-explicit and process-based C erosion dynamics model, CE-DYNAM, which simulates the redistribution of soil and C over land as a result of water erosion and calculates the role of this redistribution for C budgets at catchment scale. We demonstrate that CE-DYNAM captures the spatial variability in soil erosion, C~~arbon~~ erosion and SOC stocks of the non-Alpine region of the Rhine catchment when compared to high-resolution estimates and observations. We also show that the quantile ranges of erosion and deposition rates and C stocks fall within the uncertainty ranges of previous estimates at basin or sub-basin level. Furthermore, we demonstrate the model ability to disentangle vertical C fluxes resulting from the redistribution of C over land and develop C budgets that can shed light on the role of erosion in the C cycle. The simple structure of CE-DYNAM and the relative low amount of parameters makes it possible to run several simulations to investigate the role of individual processes on the C cycle such as removal by erosion only, or the role of deposition and transport. Its compatibility with land surface models makes it possible to investigate the long-term and large-scale effect of erosion processes under various global changes such as increasing atmospheric CO_2 concentrations, changes to precipitation and temperature, and land use change.

The application of CE-DYNAM for the Rhine catchment for the period 1850-2005 AD reveals three key findings:

- Soil erosion leads to a cumulative net C sink of 216±23 ~~90~~ Tg by the end of the period, which is in the same order of magnitude as ~~equal to one fourth of~~ the cumulative land C sink of the Rhine without erosion. This C sink is a result of an increasing dynamic replacement of C on eroding sites due to the CO_2 fertilization effect, despite

decreasing soil and C erosion rates over the largest part of the catchment. We conclude that it is important to take global changes such as climate change into account to better quantify the net effect of erosion on the C cycle.

- After performing a sensitivity analysis on key model parameters we find that the C enrichment by erosion, crop residue management and a different spatial variability of the residence time of floodplain sediment can substantially change the overall values of C fluxes and SOC storages. However, the main findings, such as soil erosion being a net C sink for the Rhine catchment, remain. ~~The erosion-induced C sink decreases over time due to decreasing erosion rates and increasing respiration of deposited C in alluvial and colluvial reservoirs. In contrast to colluvial reservoirs, alluvial reservoirs experience a net C burial. However, this net C burial can become net C respiration due to changes in the climate such as global warming. We conclude that burial of eroded C in floodplains plays an essential role in the strength of the erosion-induced C sink.~~
- Initial climate and land cover conditions and the transient period over which erosion under global changes takes place are essential for the determination if soil erosion is a net C sink or source and to what extent.

Altogether, these results indicate that despite model uncertainties related to the relative coarse spatial resolution, missing or simplified processes, CE-DYNAM represents an important step forwards into integrating soil erosion processes and sediment dynamics in Earth system models. The next step would be to improve CE-DYNAM with respect to riverine sediment and POC export fluxes and management practices.

Code and data availability

The source code of CE-DYNAM is included as a supplement to this paper. Model data can be accessed from the Zenodo repository under the doi:10.5281/zenodo.2642452 (not published yet). For the other data sets that are listed in Table 1, it is encouraged to contact the first authors of the original references.

Author contributions

VN built and implemented the mode. YW provided the basic structure for the model. All authors contributed in the interpretation of the results and wrote the paper.

Competing interests

The authors declare that they have no conflict of interest.

Acknowledgements

977 Funding was provided by the Laboratory for Sciences of Climate and Environment (LSCE), CEA, CNRS, and UVSQ.
978 Victoria Naipal, Ronny Lauerwald and Philippe Ciais acknowledges support from the VERIFY project that received
979 funding from the European Union's Horizon 2020 research and innovation program under grant agreement No 776810.
980 Bertrand Guenet acknowledges support from the project ERANETMED2-72-209 ASSESS. We also thank Dr. S. Peng for
981 sharing the PFT maps.
982
983 **References**
984
985 Asselman, N. E. M.: Suspended sediment dynamics in a large drainage basin : the River Rhine , 1450(November 1998),
986 1437–1450, https://doi.org/10.1002/(SICI)1099-1085(199907)13:10<1437::AID-HYP821>3.0.CO;2-J ,1999.
987
988 Asselman, N. E. M., Middelkoop, H. and van Dijk, P. M.: The impact of changes in climate and land use on soil erosion,
989 transport and deposition of suspended sediment in the River Rhine, Hydrol. Process., 17(16), 3225–3244,
990 doi:10.1002/hyp.1384, 2003.
991
992 Ballabio, C., Panagos, P. and Monatanarella, L.: Geoderma Mapping topsoil physical properties at European scale using the
993 LUCAS database, Geoderma, 261, 110–123, doi:10.1016/j.geoderma.2015.07.006, 2016.
994
995 Berhe, A. A., Harte, J., Harden, J. W. and Torn, M. S.: The Significance of the Erosion-induced Terrestrial Carbon Sink,
996 Bioscience, 57(4), 337, doi:10.1641/B570408, 2007.
997
998 Berhe, A. A., Harden, J. W., Torn, M. S. and Harte, J.: Linking soil organic matter dynamics and erosion-induced terrestrial
999 carbon sequestration at different landform positions, J. Geophys. Res. Biogeosciences, 113(4), 1–12,
1000 doi:10.1029/2008JG000751, 2008.
1001
1002 Beusen, A. H. W., Dekkers, A. L. M., Bouwman, A. F., Ludwig, W., & Harrison, J.: Estimation of global river transport of
1003 sediments and associated particulate C, N, and P, Global Biogeochemical Cycles, 19(4), doi:10.1029/2005GB002453,
1004 2005.
1005
1006 Billings, S. A., Richter, D. D. B., Ziegler, S. E., Prestegaard, K. and Wade, A. M.: Distinct Contributions of Eroding and
1007 Depositional Profiles to Land-Atmosphere CO2 Exchange in Two Contrasting Forests, 7(March),
1008 doi:10.3389/feart.2019.00036, 2019.
1009
1010 Borrelli, P., Van Oost, K., Meusburger, K., Alewell, C., Lugato, E., Panagos, P.:. A step towards a holistic assessment of
1011 soil degradation in Europe: Coupling on-site erosion with sediment transfer and carbon fluxes, Environmental Research,
1012 161, 291-298, doi:https://doi.org/10.1016/j.envres.2017.11.009, 2018

de Brogniez, D., Ballabio, C., Stevens, A., Jones, R. J. A., Montanarella, L. and Van Wesemael, B.: A map of the topsoil organic carbon content of Europe generated by a generalized additive model, Eur. J. Soil Sci., 66(January), 121–134, doi:10.1111/ejss.12193, 2015.

Bug, J., Stolz, W., Stegger, U.: Potentielle Erosionsgefaehrdung der Ackerboeden durch Wasser in Deutchland, Bundesanstalt fuer Geowissenschaften und Rohstoffe, www.bgr.bund.de/Boden, 2014

Cerdan, O., Govers, G., Le Bissonnais, Y., Van Oost, K., Poesen, J., Saby, N., Gobin, a., Vacca, a., Quinton, J., Auerswald, K., Klik, a., Kwaad, F. J. P. M., Raclot, D., Ionita, I., Rejman, J., Rousseva, S., Muxart, T., Roxo, M. J. and Dostal, T.: Rates and spatial variations of soil erosion in Europe: A study based on erosion plot data, Geomorphology, 122(1–2), 167–177, doi:10.1016/j.geomorph.2010.06.011, 2010.

Ciais, P., Sabine, C., Bala, G., Bopp, L., Brovkin, V., Canadell, J., Chhabra, A., DeFries, R., Galloway, J., Heimann, M., Jones, C., Quéré, C. Le, Myneni, R. B., Piao, S. and Thornton, P.: Carbon and Other Biogeochemical Cycles, in Climate Change 2013: The physical science basis. Contribution of working group I to the fifth assessment report of the intergovernmental panel on climate change [Stocker, T.F., D. Qin, G.-K. Plattner, M. Tignor, S.K. Allen, J. Boschung, A. Nauels, Y. Xia, pp. 465–570, Cambridge University Press, Cambridge, United Kingdom and New York, NY., 2013.

De Moor, J. J. W., & Verstraeten, G.: Alluvial and colluvial sediment storage in the Geul River catchment (The Netherlands)—combining field and modelling data to construct a Late Holocene sediment budget, Geomorphology, *95*(3-4), 487-503, 2008.

Doetterl, S., Van Oost, K. and Six, J.: Towards constraining the magnitude of global agricultural sediment and soil organic carbon fluxes, Earth Surf. Process. Landforms, doi:10.1002/esp.3198, 2012.

Doetterl, S., Berhe, A. A., Nadeu, E., Wang, Z., Sommer, M., & Fiener, P.: Erosion, deposition and soil carbon: a review of process-level controls, experimental tools and models to address C cycling in dynamic landscapes, Earth-Science Reviews, 154, 102-122, 2016.

Dotterweich, M.: Geomorphology The history of human-induced soil erosion : Geomorphic legacies , early descriptions and research , and the development of soil conservation — A global synopsis, Geomorphology, 201(November), 1–34, doi:10.1016/j.geomorph.2013.07.021, 2013.

Elliot, W. J.: WEPP INTERNET INTERFACES FOR FOREST EROSION PREDICTION 1, JAWRA Journal of the American Water Resources Association, *40*(2), 299-309, 2004.

Erkens, G.: Sediment dynamics in the Rhine catchment, Utrecht University, Faculty of Geosciences, Utrecht., 2009.

Foster, G. R., Yoder, D. C., Weesies, G. A., McCool, D. K., McGregor, K. C., & Bingner, R. L: User's Guide—revised universal soil loss equation version 2 (RUSLE 2). USDA–Agricultural Research Service, Washington, DC., *2002*

Frieler, K., Lange, S., Piontek, F., Reyer, C. P. O., Schewe, J., Warszawski, L., Zhao, F., Chini, L., Denvil, S., Emanuel, K., Geiger, T., Halladay, K., Hurtt, G., Mengel, M., Murakami, D., Ostberg, S., Popp, A. and Riva, R.: Assessing the impacts of 1 . 5 ◦ C global warming – simulation protocol of the Inter-Sectoral Impact Model Intercomparison Project (ISIMIP2b), Geosci. Model Dev., 10, 4321–4345, 2017.

Galy, V., Peucker-Ehrenbrink, B., & Eglinton, T. Global carbon export from the terrestrial biosphere controlled by erosion. Nature, 521, 204–207.https://doi.org/10.1038/nature14400, 2015.

Guenet, B., Camino-Serrano, M., Ciais, P., Tifafi, M., Maignan, F., Soong, J. L., & Janssens, I. A.: Impact of priming on global soil carbon stocks, Global change biology, 24(5), 1873-1883, 2018.

Gumiere, S. J., Le Bissonnais, Y., Raclot, D., & Cheviron, B.: Vegetated filter effects on sedimentological connectivity of agricultural catchments in erosion modelling: a review. *Earth Surface Processes and Landforms*, *36*(1), 3-19, 2011.

Hay R.K.M.: Harvest index: a review of its use in plant breeding and crop physiology, Ann. appl. Biol., 126, 197–216, 1995.

Hoffmann, T., Erkens, G., Cohen, K. M., Houben, P., Seidel, J. and Dikau, R.: Holocene floodplain sediment storage and hillslope erosion within the Rhine catchment, The Holocene, 17(1), 105–118, doi:10.1177/0959683607073287, 2007.

Hoffmann, T., Lang, a and Dikau, R.: Holocene river activity: analysing 14C-dated fluvial and colluvial sediments from Germany, Quat. Sci. Rev., 27(21–22), 2031–2040, doi:10.1016/j.quascirev.2008.06.014, 2008.

Hoffmann, T., Schlummer, M., Notebaert, B., Verstraeten, G. and Korup, O.: Carbon burial in soil sediments from Holocene agricultural erosion, Central Europe, Global Biogeochem. Cycles, 27(3), 828–835, doi:10.1002/gbc.20071, 2013a.

Hoffmann, T., Mudd, S. M., van Oost, K., Verstraeten, G., Erkens, G., Lang, a., Middelkoop, H., Boyle, J., Kaplan, J. O., Willenbring, J. and Aalto, R.: Short Communication: Humans and the missing C-sink: erosion and burial of soil carbon through time, Earth Surf. Dyn., 1(1), 45–52, doi:10.5194/esurf-1-45-2013, 2013b.

Hurtt, G. C., Chini, L. P., Frolking, S., Betts, R. A., Feddema, J. and Fischer, G.: Harmonization of land-use scenarios for the period 1500 – 2100 : 600 years of global gridded annual land-use transitions , wood harvest , and resulting secondary lands, Clim. Chang., 109, 117–161, doi:10.1007/s10584-011-0153-2, 2011.

Kinnell, P. I. A.: Runoff dependent erosivity and slope length factors suitable for modelling annual erosion using the Universal Soil Loss Equation. Hydrological Processes: An International Journal, 21(20), 2681-2689, 2007.

Krinner, G., Viovy, N., de Noblet-Ducoudré, N., Ogée, J., Polcher, J., Friedlingstein, P., Ciais, P., Sitch, S. and Prentice, I. C.: A dynamic global vegetation model for studies of the coupled atmosphere-biosphere system, Global Biogeochem. Cycles, 19(1), 1–33, doi:10.1029/2003GB002199, 2005.

Lal, R.: Soil erosion and the global carbon budget., Environ. Int., 29(4), 437–50, doi:10.1016/S0160-4120(02)00192-7, 2003.

Lehner, B. and Grill, G.: Global river hydrography and network routing : baseline data and new approaches to study the world ' s large river systems, Hydrol. Process., 2186(April), 2171–2186, doi:10.1002/hyp.9740, 2013.

Ludwig, W. and Probst, J.-L.: River Sediment Discharge to the Oceans: Present-Day Controls and Global Budgets, Am. J. Sci., 298(April), 265–295, 1998.

Lugato, E., Smith, P., Borrelli, P., Panagos, P., Ballabio, C., Orgiazzi, A., Fernandez-ugalde, O., Montanarella, L. and Jones, A.: Soil erosion is unlikely to drive a future carbon sink in Europe, Sci. Adv., 4(November), eaau3523, 2018.

Martínez-mena, M., Almagro, M., García-franco, N., Vente, J. De and García, E.: Fluvial sedimentary deposits as carbon sinks : organic carbon pools and stabilization mechanisms across a Mediterranean catchment, 1035–1051, 2019.

Mayorga, E., Seitzinger, S. P., Harrison, J. a., Dumont, E., Beusen, A. H. W., Bouwman, a. F., Fekete, B. M., Kroeze, C. and Van Drecht, G.: Global Nutrient Export from WaterSheds 2 (NEWS 2): Model development and implementation, Environ. Model. Softw., 25(7), 837–853, doi:10.1016/j.envsoft.2010.01.007, 2010.

Müller, C., Elliott, J., Kelly, D., Arneth, A., Balkovic, J., Ciais, P., ... & Jones, C. D.: The Global Gridded Crop Model Intercomparison phase 1 simulation dataset, Scientific data, 6(1), 50, 2019.

Nadeu, E., Gobin, A., Fiener, P., van Wesemael, B. and van Oost, K.: Modelling the impact of agricultural management on soil carbon stocks at the regional scale: the role of lateral fluxes., Glob. Chang. Biol., 21(8), 3181–92,

doi:10.1111/gcb.12889, 2015.

Naipal, V., Reick, C., Pongratz, J. and Van Oost, K.: Improving the global applicability of the RUSLE model - Adjustment of the topographical and rainfall erosivity factors, Geosci. Model Dev., 8(9), doi:10.5194/gmd-8-2893-2015, 2015.

Naipal, V., Reick, C., Van Oost, K., Hoffmann, T. and Pongratz, J.: Modeling long-term, large-scale sediment storage using a simple sediment budget approach, Earth Surf. Dyn., 4, 407–423, doi:10.5194/esurf-4-407-2016, 2016.

Naipal, V., Ciais, P., Wang, Y., Lauerwald, R., Guenet, B. and Oost, K. Van: Global soil organic carbon removal by water erosion under climate change and land use change during AD 1850 – 2005, Biogeosciences, 15(July), 4459–4480, doi:https://doi.org/10.5194/bg-15-4459-2018, 2018.

Van Oost, K., Quine, T. a, Govers, G., De Gryze, S., Six, J., Harden, J. W., Ritchie, J. C., McCarty, G. W., Heckrath, G., Kosmas, C., Giraldez, J. V, da Silva, J. R. M. and Merckx, R.: The impact of agricultural soil erosion on the global carbon cycle., Science, 318(5850), 626–9, doi:10.1126/science.1145724, 2007.

Van Oost, K., Verstraeten, G., Doetterl, S., Notebaert, B., Wiaux, F. and Broothaerts, N.: Legacy of human-induced C erosion and burial on soil – atmosphere C exchange, PNAS, 109(47), 19492–19497, doi:10.1073/pnas.1211162109/-/DCSupplemental.www.pnas.org/cgi/doi/10.1073/pnas.1211162109, 2012.

Palmieri, A., Martino, L., Dominici, P. and Kasanko, M.: Land Cover and Land Use Diversity Indicatorsin LUCAS 2009 data., 2011.

Panagos, P., Borrelli, P., Poesen, J., Ballabio, C., Lugato, E., Meusburger, K., Montanarella, L. and Alewell, C.: Environmental Science & Policy The new assessment of soil loss by water erosion in Europe, Environ. Sci. Policy, 54, 438–447, doi:10.1016/j.envsci.2015.08.012, 2015.

Panagos, P., Borrelli, P., Meusburger, K., Yu, B., Klik, A., Lim, K. J., Yang, J. E., Ni, J., Miao, C., Chattopadhyay, N., Sadeghi, S. H., Hazbavi, Z., Zabihi, M., Larionov, G. A., Krasnov, S. F., Gorobets, A. V., Levi, Y., Erpul, G., Birkel, C., Hoyos, N., Naipal, V., Oliveira, P. T. S., Bonilla, C. A., Meddi, M., Nel, W., Al Dashti, H., Boni, M., Diodato, N., Van Oost, K., Nearing, M. and Ballabio, C.: Global rainfall erosivity assessment based on high-temporal resolution rainfall records, Sci. Rep., 7(1), doi:10.1038/s41598-017-04282-8, 2017.

Parton, W. J., Schimel, D. S., Cole, C. V. and Ojima, D. S.: Analysis of Factors Controlling Soil Organic Matter Levels in Great Plains Grasslands1, Soil Sci. Soc. Am. J., 51(5), 1173, doi:10.2136/sssaj1987.03615995005100050015x, 1987.

Pelletier, J. D.: A spatially distributed model for the long-term suspended sediment discharge and delivery ratio of drainage basins,J. Geophys. Res., *Earth Surface* 117 (F2), doi: https://doi.org/10.1029/2011JF002129, 2012.

Pelletier, J. D., Broxton, P. D., Hazenberg, P., Zeng, X., Troch, P. A., Niu, G. Y., Williams, Z., Brunke, M. A. and Gochis, D.: A gridded global data set of soil, intact regolith, and sedimentary deposit thicknesses for regional and global land surface modeling, J. Adv. Model. Earth Syst., doi:10.1002/2015MS000526, 2016.

Peng, S., Ciais, P., Maignan, F., Li, W., Chang, J., Wang, T. and Yue, C.: Sensitivity of land use change emission estimates to historical land use and land cover mapping, Global Biogeochem. Cycles, 31(4), 626–643, doi:10.1002/2015GB005360, 2017.

Renard, K. G., & Ferreira, V. A.: RUSLE model description and database sensitivity. Journal of environmental quality, 22(3), 458-466, 1993.

Renard, K.G., Foster, G.R., Weesies, G.A., McCool, D.K., Yoder, D. C.: Predicting Soil Erosion by Water: A Guide to Conservation Planning with the Revised Universal Soil Loss Equation (RUSLE), United States Department of Agriculture, Washington, DC., 1997.

Schauberger, B., Ben-ari, T., Makowski, D., Kato, T., Kato, H. and Ciais, P.: Yield trends , variability and stagnation analysis of major crops in France over more than a century, Sci. Rep., (November), 1–12, doi:10.1038/s41598-018-35351-1, 2018.

Shangguan H.W., Dai Y., Duan Q., Liu B., Y. H.: A global soil data set for earth system modeling Wei, J. Adv. Model. Earth Syst., 6, 249–263, 2014, doi:10.1002/2013MS000293.

Sorribas, M. V., da Motta Marques, D., Castro, N. M. D. R., & Fan, F. M.: Fluvial carbon export and CO2 efflux in representative nested headwater catchments of the eastern La Plata River Basin, Hydrological processes, 31(5), 995-1006, 2017.

Stallard, R. F.: Terrestrial sedimentation and the carbon cycle : Coupling weathering and erosion to carbon burial, Global Biogeochem. Cycles, 12(2), 231–257, 1998.

Tan, Z., Leung, L. R., Li, H., Tesfa, T., Vanmaercke, M., Poesen, J., ... Hartmann, J. A Global data analysis for representing sediment and particulate organic C carbon yield in Earth System Models. Water Resources Research, 53, 10,674–10,700. https://doi.org/10.1002/2017WR020806, 2017

Thonicke, K., Spessa, A., Prentice, I. C., Harrison, S. P. and Dong, L.: The influence of vegetation , fire spread and fire behaviour on biomass burning and trace gas emissions : results from a process-based model, Biogeosciences, 7, 1991–2011, doi:10.5194/bg-7-1991-2010, 2010.

Todd-Brown, K. E., Randerson, J. T., Post, W. M., Hoffman, F. M., Tarnocai, C., Schuur, E. A., & Allison, S. D.: Causes of variation in soil carbon simulations from CMIP5 Earth system models and comparison with observations, Biogeosciences (10), 1717-1736, 10.5194/bg-10-1717-2013, 2013.

Wang, Z., Govers, G., Steegen, A., Clymans, W., Putte, A. Van Den, Langhans, C., Merckx, R. and Oost, K. Van: Geomorphology Catchment-scale carbon redistribution and delivery by water erosion in an intensively cultivated area, Geomorphology, 124(1–2), 65–74, doi:10.1016/j.geomorph.2010.08.010, 2010.

Wang, Z., Doetterl, S., Vanclooster, M., van Wesemael, B. and Van Oost, K.: Constraining a coupled erosion and soil organic carbon model using hillslope-scale patterns of carbon stocks and pool composition, J. Geophys. Res. Biogeosciences, 120, 452–465, doi:10.1002/2014JG002768, 2015.

Wang, Z., Hoffmann, T., Six, J., Kaplan, J. O., Govers, G., Doetterl, S. and Van Oost, K.: Human-induced erosion has offset one-third of carbon emissions from land cover change, Nat. Clim. Chang., 7(5), 345–349, doi:10.1038/nclimate3263, 2017.

Wiesmeier, M., Sporlein, P., Geuß, U. W. E., Hangen, E., Haug, S., Reischl, A., Schilling, B., Lutzow, M. V. O. N. and Kogel-Knaber, I.: Soil organic carbon stocks in southeast Germany (Bavaria) as affected by land use , soil type and sampling depth, Glob. Chang. Biol., (March), 1–13, doi:10.1111/j.1365-2486.2012.02699.x, 2012.

Table 1: Model input datasets

Dataset	Spatial resolution	Temporal resolution	Period	Source
Historical land cover and land use change	0.25 degrees	annual	1850-2005	Peng et al. (2017)
Climate data (precipitation & temperature) for ORCHIDEE	0.5 degrees	6 hourly	1900-2012	CRU-NCEP version 5.3.2; https://crudata.uea.ac.uk/cru/data/ncep/; last access: 5 April 2019
precipitation for the Adj. RUSLE	0.5 degrees	monthly	1850-2005	ISIMIP2b (Frieler et al., 2017)
Soil	1 km	-	-	Global Soil Dataset for Earth System Modeling, GSDE (Shangguan H.W., Dai Y., Duan Q., Liu B., 2014)
Topography	30 arcseconds	-	-	GTOPO30; U.S. Geological Survey, EROS Data Center Distributed Active Archive Center 2004; https://www.ngdc.noaa.gov/mgg/topo/gltiles.html; last access: 5 April 2019
Flow accumulation	30 arcseconds	-	-	HydroSHEDS (Lehner et al., 2013); https://www.hydrosheds.org/; last access: 5 April 2019
Hillslopes/Floodplain area	5 arcminutes	-	-	Pelletier et al. (2016)
River network & stream length	30 arcseconds	-	-	Hydrosheds (Lehner et al., 2008)

Table 2: Model simulations, with changes to the basin average gross soil erosion rate (t ha^{-1} y^{-1}), the basin average sediment residence time Tau (years), and the enrichment factor, and the crop residue harvest intensity, RM (%).

Default simulations	Gross soil erosion	Tau	Enrichment factor	RM
S0	0	-	-	0
S1	3.94	94	1	0
S2	3.94	94	1	0
Uncertainty simulations				
S1_min	1.52	94	1	0
S2_min	1.52	94	1	0
S1_max	5.95	94	1	0
S2_max	5.95	94	1	0
Sensitivity				

simulations				
S2_Tmin	3.94	60	1	0
S2_Tmax	4.94	128	1	0
S1_EF	5.94	94	2	0
S2_EF	6.94	94	2	0
S0_RM	0	-	-	100
S1_RM	3.94	94	1	100
S2_RM	3.94	94	1	100

Table 3: Goodness-of-fit results of the comparison of the simulated gross and net erosion rates to those of other studies at subbasin level, taking into account 13 sub-basins of the Rhine. RMSE is the root mean square error in 10^6 tons $year^{-1}$. E stands for soil erosion.

	E Cerdan et al. (2010)	E Germany	E RUSLE2015	E Borrelli et al. (2018)
r-squared	0.72	0.97	0.94	0.24
RMSE	0.68	1.98	0.92	1.35

Table 4: Goodness-of-fit results of the comparison of the simulated gross and net C erosion rates to those of the study of Lugato et al. (2018) in the enhanced and reduced scenario, taking into account 13 sub-basins of the Rhine. RMSE is the root mean square error in tons $year^{-1}$. Ce stands for gross C erosion, while Cd stands for net C erosion.

	Ce enhanced	Ce reduced	Cd enhanced	Cd reduced
r-squared	0.95	0.95	0.98	0.98
RMSE	7977	13797	3450	9822

Table 5: This table shows the results of the linear regression between the simulated total SOC stocks (Tg of C per year) and those of the Global Soil dataset for Earth System Modeling (GSDE) and from the LUCAS database. The regression is done after aggregating the data at sub-basin level for the 13 sub-basins that were delineated in the Rhine catchment. RMSE is the root mean square error given in Tg of C per year, while the r-value is the spatial correlation coefficient.

Regression	r-value	p-value	RMSE
This study versus LUCAS	0.96	<0.01	28.69
This study versus GSDE	0.95	<0.01	29.32

Table 64: This table presents the scaling exponent (b) of equation 20 for floodplains and hillslopes. The scaling exponent was derived for selected points in the Rhine catchment for which measurements on the SOC storage were taken by Hoffmann et al. (2013), and at sub-basin level after the data on area and SOC stocks was aggregated for each of the 13 sub-basins of the Rhine.

	Scaling exponent floodplains	Scaling exponent hillslopes
Hoffmann et al. (2013)	1.23±0.06	1.08±0.07
This study (selected points where measurements were taken)	1.14	0.83
This study (based on the 13 sub-basins)	1.06	1.00

Table 7: Sensitivity analysis. The impacts of enrichment, changes to the sediment residence time (τmin, τmax), and crop residue management (RM) on the cumulative gross C erosion (C_e), the cumulative change in the total SOC stock ($dSOC$), the net C sink and the cumulative particulate organic C export flux (POC_{exp}) of the Rhine catchment. Units: Tg C

	C_e	**dSOC**	**C sink/source**	**POC_{exp}**
Default	66	142	216	0.138
enrichment	106	198	271	0.137
τmin	66	130	204	0.198
τmax	66	100	173	0.117
RM	52	105	194	0.134

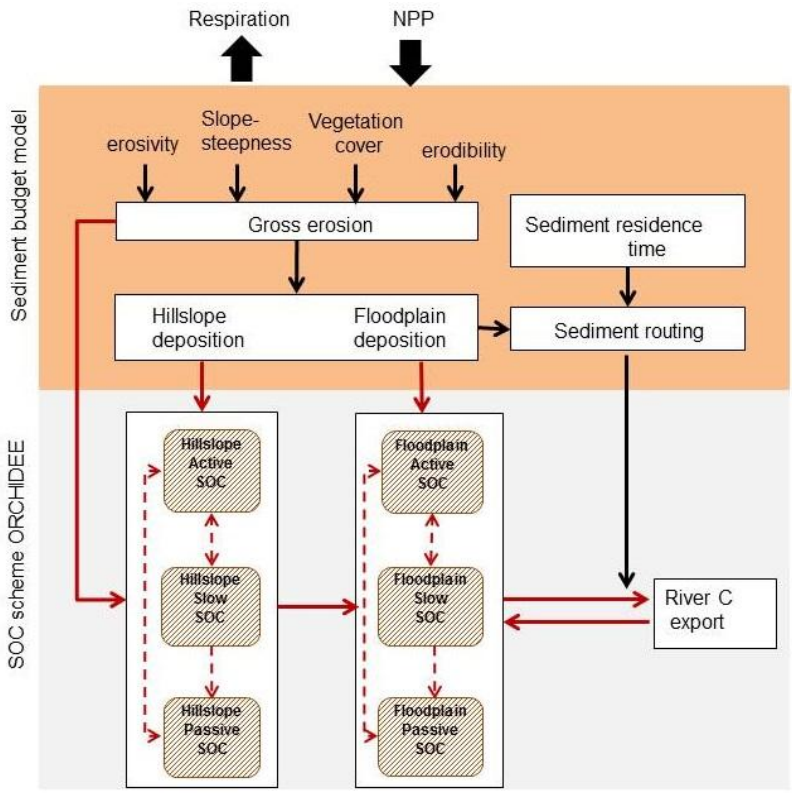

Figure 1: A conceptual diagram of CE-DYNAM. The red arrows represent the C fluxes between the C pools/reservoirs, while the black arrows represent the link between the erosion processes (removal, deposition and transport).

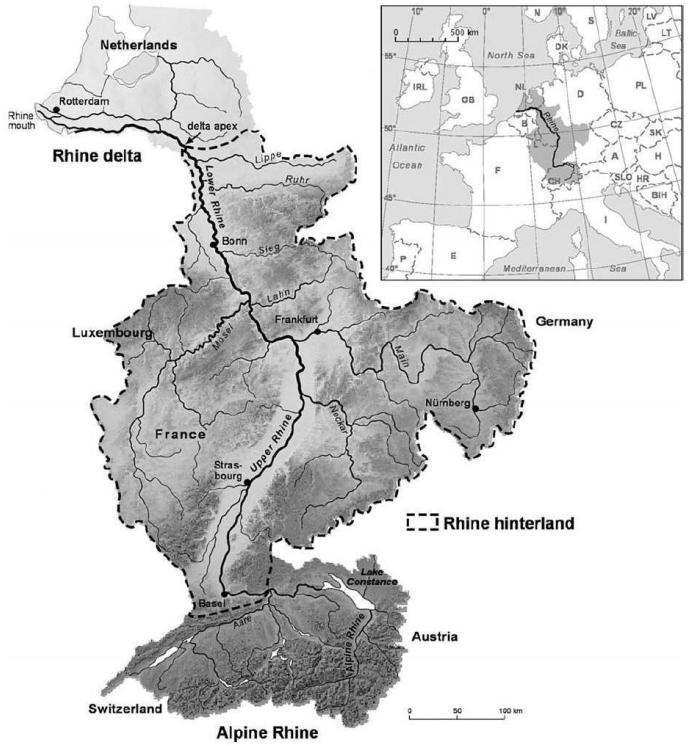

Figure 2: The Rhine catchment (Hoffmann et al., 2013), where the gray shades represent elevation and the continues black lines the main rivers.

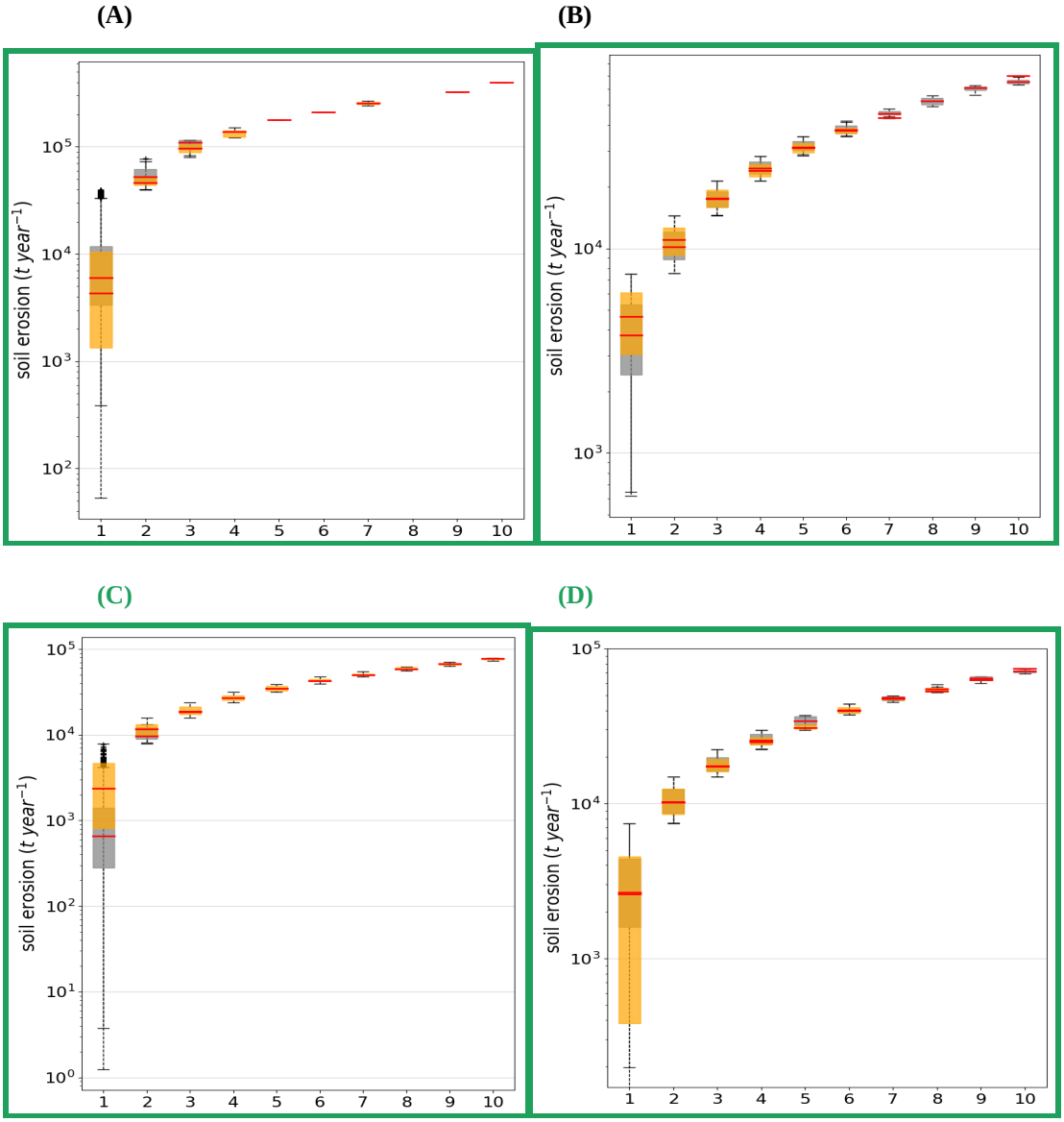

Figure 3: Quantile-whisker plot of simulated **gross** soil erosion rates (t/year) (grey whisker boxes), compared to (A) the study of Cerdan et al. (2010), ~~and~~ (B) the study of Panagos et al. (2015), and (C) the German potential erosion map by Bug et al. (2014) (orange whisker boxes). (D~~E~~) Quantile-whisker plot of simulated **net** soil erosion rates (t/year) (grey whisker boxes), compared to the study of Borrelli et al. (2018) (orange whisker boxes). Medians are plotted as red horizontal lines. The x-axis represents bins or evenly spaced ranges between the minimum and maximum total yearly soil erosion rates of the Rhine.

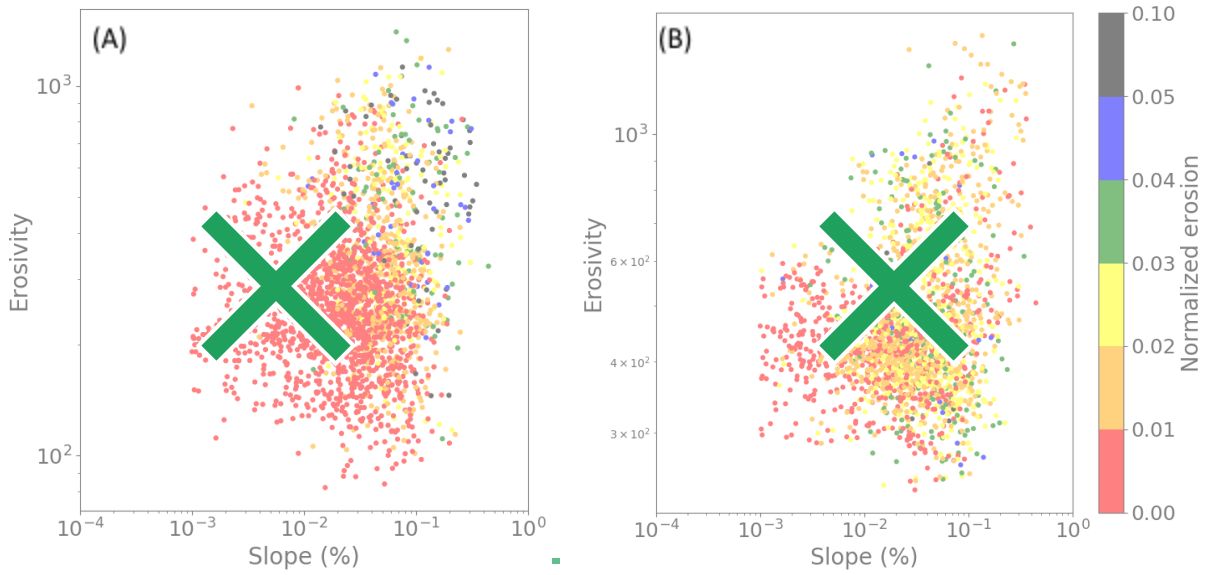

Figure 4: Normalized gross soil erosion as a function of the topographical slope (%) and rainfall erosivity for (A) this study and (B) RUSLE2015

(A) **(B)**

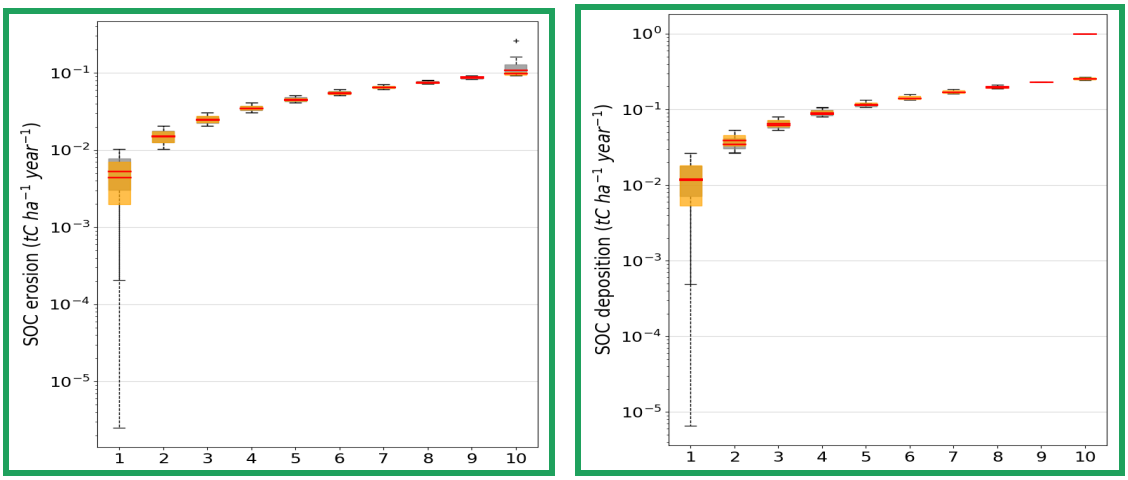

(C) **(D)**

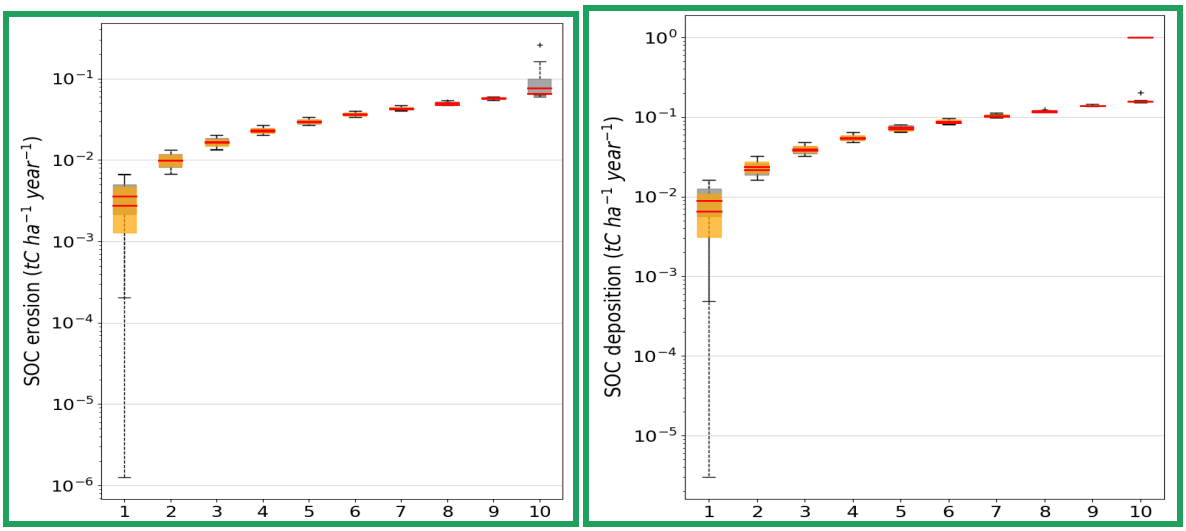

Figure 45: (A) Hillslope C erosion rates and, (B) C deposition rates, compared to the enhanced erosion scenario from Lugato et al. (2018). (C) Hillslope C erosion rates and, (D) C deposition rates, compared to the reduced erosion scenario from Lugato et al. (2018). The x-axis represents bins or evenly spaced ranges between the minimum and maximum total yearly soil erosion rates of the Rhine.

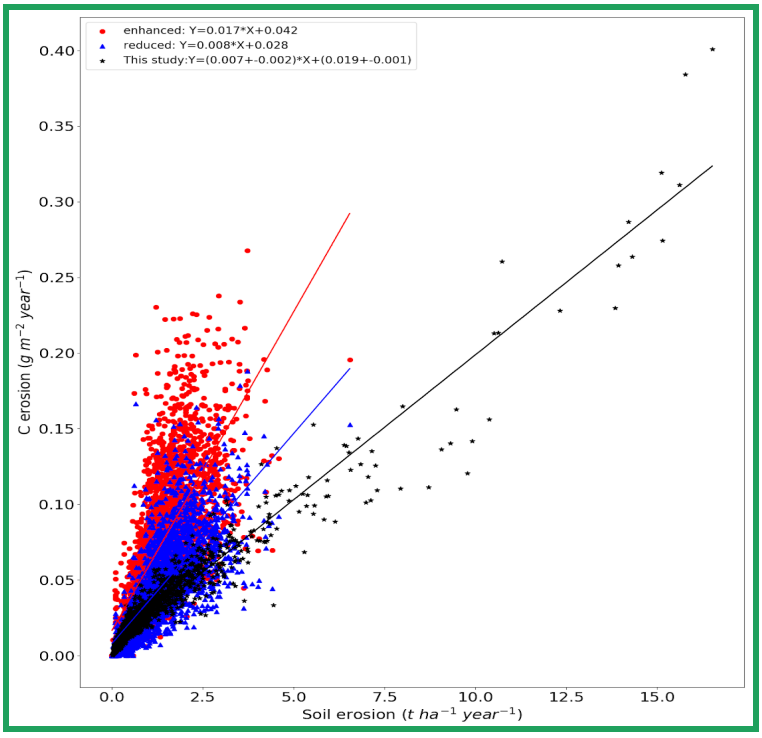

Figure 56: The relationship between soil erosion and C erosion of simulation S2 (blackstars~~points~~) in comparison to the erosion scenarios from the study of Lugato et al. (2018) with enhanced (red circles~~points~~) and reduced erosion (blue triangles~~points~~), respectively. The straight lines are the trendlines of the linear regression between soil and C erosion.

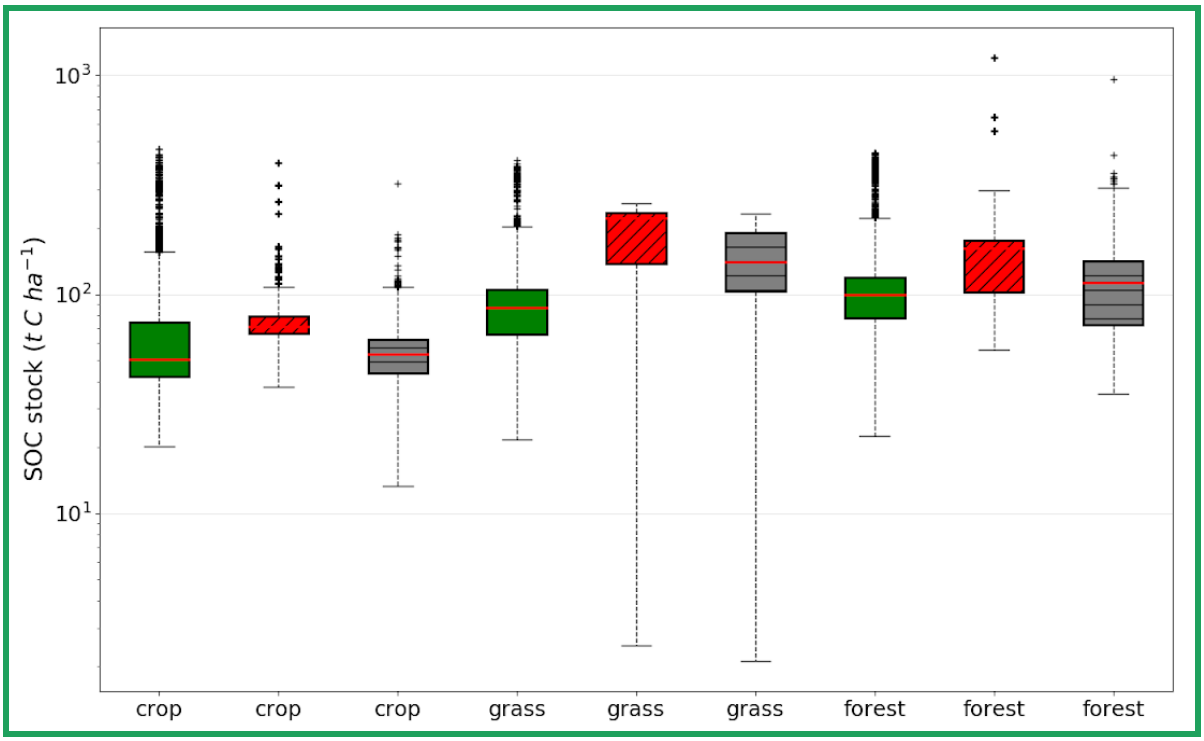

Figure 67: Comparison of the total SOC stocks per land cover type between the simulation without erosion (red boxes with a '//' pattern), the simulation with erosion (black boxes with a '-' pattern) and the LUCAS data (green boxes without pattern fill). The red horizontal lines are the medians~~, the blue stars are the means~~, the dashed vertical lines represent the range between the minimum and maximum, and the black dots are the outliers.

(A) **(B)**

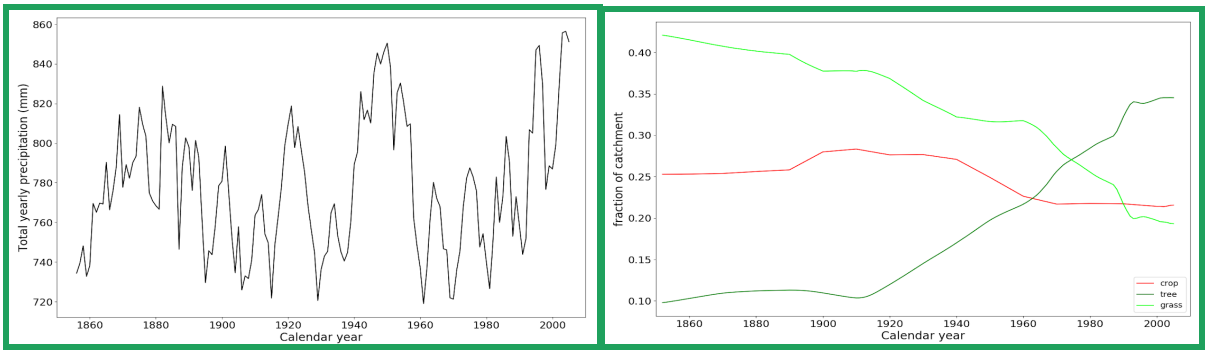

(C) **(D)**

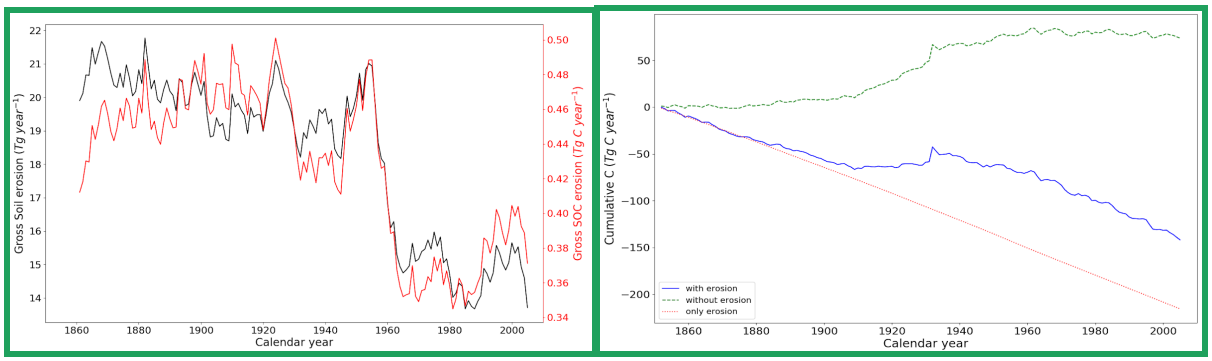

Figure 78: Timeseries of (A) the 5-year average yearly precipitation ~~of the entire Rhine catchment~~ (mm), (B) changing land cover fractions ~~of the entire Rhine catchment~~, (C): 5-year average ~~of the~~ total gross soil erosion (Pg year^{-1}) and total gross C erosion rates (Tg C year^{-1}) ~~of the **entire Rhine** catchment~~, (D): ~~5-year average of the total gross soil erosion (Pg year^{-1}) and C erosion rates (Tg C year^{-1}) of the **non-Alpine region** of the Rhine. Erosion on bare soil is not taken into account here. (E)~~ Cumulative C emissions from the soil to the atmosphere under land use change and climate change without soil erosion (green dashed line~~F_atm0~~), with soil erosion (blue straight line~~F_atm1~~), due to additional respiration or stabilization of buried soil and photosynthetic replacement of C under erosion (Ep, red dotted line). All graphs represent the non-Alpine region of the Rhine catchment.

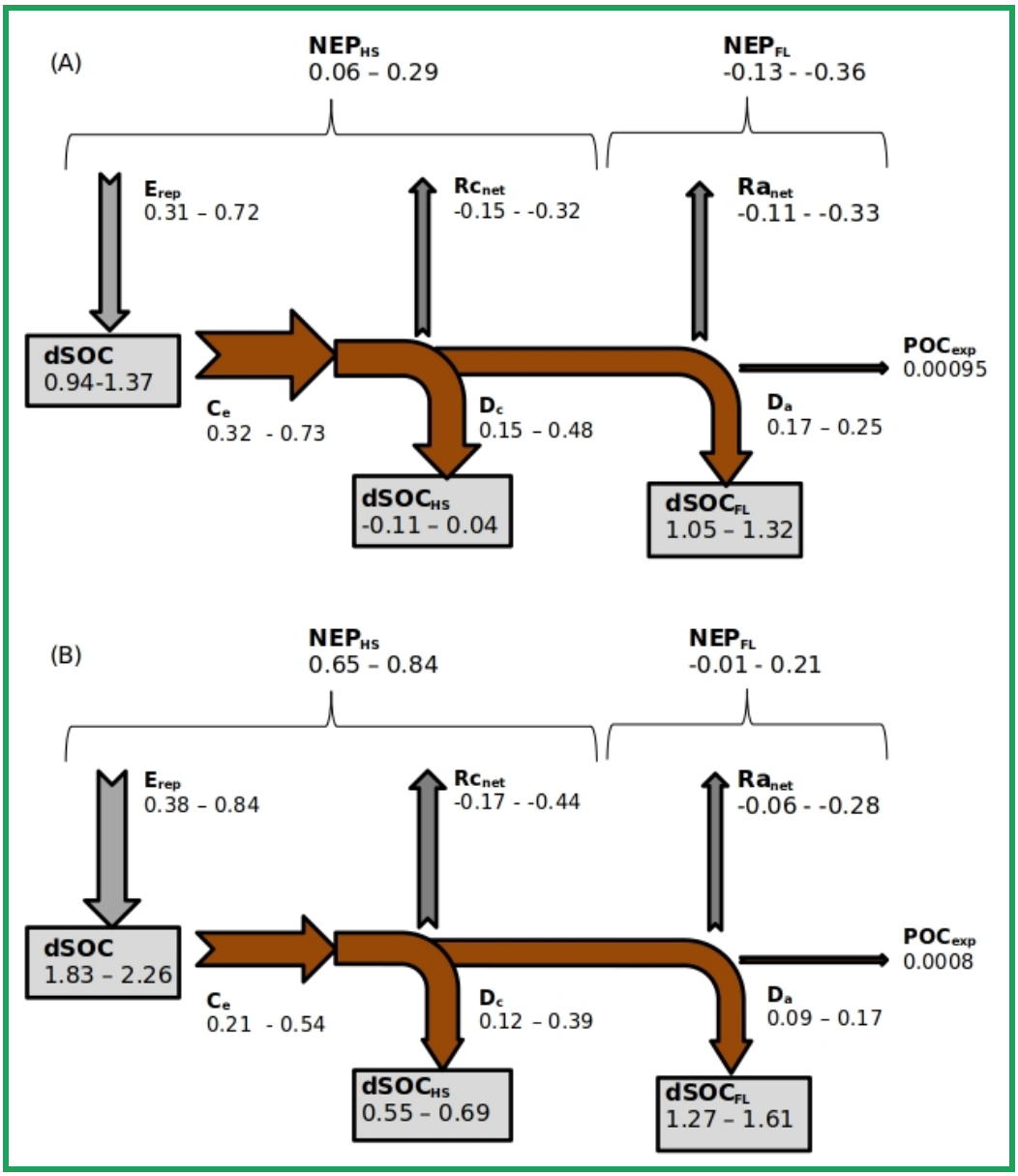

Figure 89: (A) C budget of the non-Alpine part of the ~~entire~~ Rhine for the period 1851-1861, and (B) for the period 1995-2005. The budget shows the net exchange of C (Tg C year^{-1}) between the soil and atmosphere as a result of accelerated soil erosion rates. Grey arrows are the erosion-induced yearly average **vertical** C fluxes, while the brown arrows are the erosion-induced yearly average **lateral** C fluxes. ~~The grey boxes represent yearly average changes in SOC stocks for the specific time period as a result of land use change, climate change, erosion and deposition.~~ C_e: Gross C erosion from hillslopes; D_c: Deposition of C on hillslopes; D_a: Deposition of C in floodplains; POC_{exp}: net POC export flux; E_p: Erosion-induced C replacement on hillslopes (Eq. 21); Ra_{net}: Net respiration/burial of deposited C in floodplains (Eq. 23); Rc_{net}: Net respiration/burial of deposited C on hillslopes (Eq. 22); NEP_{HS}: Net ecosystem productivity of hillslopes;

NEP_{FL}: Net ecosystem productivity of floodplains; The grey boxes represent yearly average changes in SOC stocks for the specific time period as a result of land use change, climate change, erosion and deposition. *dSOC*: Yearly average change in the total SOC stock; $dSOC_{HS}$: Yearly average change in the hillslope SOC stock; $dSOC_{FL}$: Yearly average change in the floodplain SOC stock.

(A) **(B)**

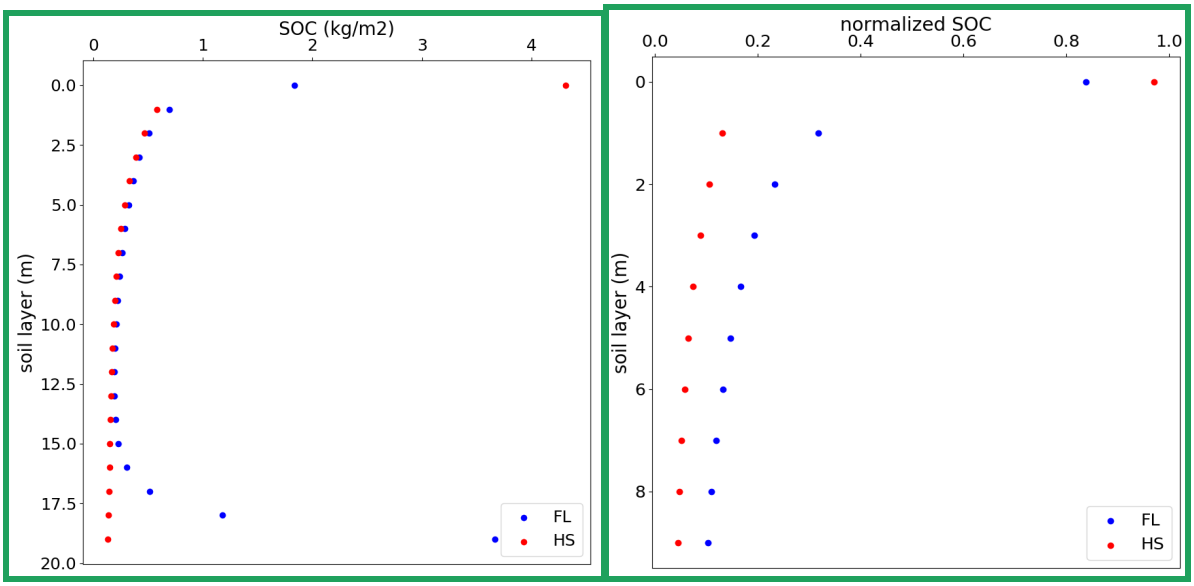

Figure ~~9~~10: (A) Vertical distribution of hillslope (red) and floodplain (blue) SOC stocks (kg m^{-2}) with depth averaged over the non-Alpine region of the ~~whole~~ Rhine catchment, and (B) the vertical distribution of normalized hillslope (red) and floodplain (blue) SOC stocks (dimensionless) with depth ~~averaged over the whole Rhine catchment~~.